Quarterly Report

on

Long Endurance Underwater Power System

April 1989 - June 1989

Contract No. N00014-87-C-0335

Aquanautics Corporation
980 Atlantic Avenue, #101
Alameda, CA 94501
August 4, 1989

Approved for Public Release
Distribution Unlimited

2.0 AQUANAUTICS POWER SOURCE

2.1 Concept

As part of DARPA's "Artificial Gill" program, Aquanautics is developing an underwater power source that is at least 2 to 3 times more efficient than lithium thionyl chloride. It uses an ambient pressure solid polymer electrolyte (SPE) hydrogen/oxygen fuel cell with an artificial gill that extracts dissolved oxygen from seawater and an Alwatt aluminum corrosion cell that generates the hydrogen. The particular innovation in this concept is a direct carrier feed fuel cell (CFFC) process which allows the fuel cell to operate at ambient pressure without a costly deep water pressure vessel.

Figure 2.1 shows the schematic diagram for this system:

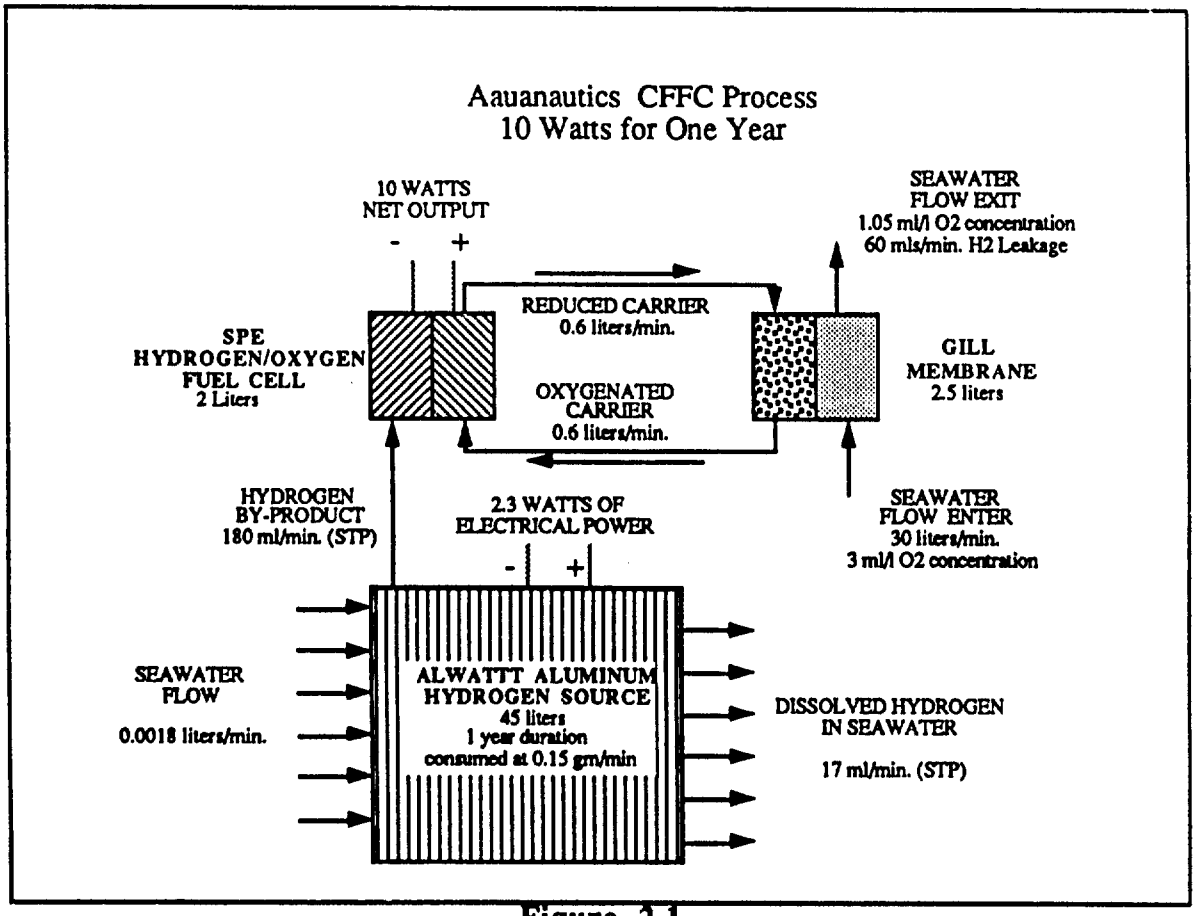

Figure 2.1

In this scheme three basic units are required which are discussed in detail below:

1. Artificial Gill
2. Hybrid Fuel Cell
3. Alwatt Hydrogen Generator

THE ARTIFICIAL GILL

The objective of the artificial gill process is to extract and concentrate the oxygen that is dissolved in the seawater rather than split the water molecule into its oxygen and hydrogen components (electrolysis). The later process requires more energy than can be recovered from burning the oxygen in a combustion process. The artificial gill requires only about 10% of the power that can be generated from the extracted oxygen in a combustion process. This factor makes a gill the the only feasible alternative for on-site oxygen production involving a power system.

The driving force for oxygen diffusion is the difference in oxygen concentration between the seawater and carrier. A membrane is used to keep these fluids separated. When the oxygen gas diffuses across the membrane from the seawater into the carrier fluid, it binds to an oxygen carrying molecule. In this bound state, the carrier fluid does not have any oxygen partial pressure. Therefore, the driving force for the oxygen diffusion is at its maximum, equal to the partial pressure of the oxygen in the seawater.

Worst case design conditions are used for the gill which assume oxygen dissolved in seawater at a concentration of approximately 1 to 3 ml per liter of seawater (see Appendix G for measured values in all the oceans).

Proper packaging of the membrane is essential to provide:

i) low volume per unit quantity of oxygen transferred
ii) low seawater drag losses
iii) low carrier pumping cost

Fortunately, the chemical industry has developed a wide range of membrane polymers that will work for underwater systems. Analysis by Aquanautics has concluded that a rectangular gill package with a hollow fiber membrane will be the best design choice with carrier flowing inside the hollow fiber and seawater flowing outside. The details of this analysis can be found in Appendix B.

THE FUEL CELL

Fuel cells are very efficient at converting the chemical energy stored as hydrogen and oxygen into electrical energy. The problem with using fuel cells at great water depth is finding an efficient means of storing the gaseous reactants and releasing them into high ambient pressures. A solution is to place the fuel cell in a pressure vessel. But at 6,000 meters such an enclosure would be very heavy and expensive. This problem has limited fuel cells from serious consideration for ocean bottom applications.

The use of an artificial gill poses a different kind of problem. Oxygen dissolved in seawater can exist in equilibrium with the maximum partial pressure of 0.2 atmospheres or 3 psi. Extracting oxygen in its gaseous form and compressing it to above ambient pressure would involve a large expenditure of power which defeats the purpose of extraction. In order to enable efficient operation at ambient pressure, it is desirable to use the oxygen while it is still in its bound state and skip the intermediate step of converting it into a gas.

The Aquanautics' gill process employs oxygen carrying molecules which can be electrochemically modulated to release the bound oxygen. Since a fuel cell is also an electrochemical system, Aquanautics has shown that the oxygen can be reduced directly at the fuel cell cathode by flowing the oxygen-rich carrier fluid through the fuel cell electrode.

This allows the fuel cell to remain at ambient pressure while eliminating the inefficient concentration or compression of the extracted oxygen.

This direct carrier feed fuel cell (CFFC) is a new development in DARPA's artificial gill program which re-introduces the possibility of using fuel cells for underwater power generation.

The exact chemical reaction mechanism is not yet known, but the overall reaction is:

$$(LM)_2 - O_2 + 2H_2O + 4e^- \text{ ---> } 2LM + 4OH^-$$

where $(LM)_2 - O_2$ is oxygenated carrier, and
LM is deoxygenated carrier

To counteract the OH^- generated, electrochemical oxidation of hydrogen is employed on the other side of a cation-exchange membrane. The hydrogen ion generated is transported across the membrane and neutralizes the OH^-.

The reaction at the anode is,

$$2H_2 \text{ ---> } 4H^+ + 4e^-$$

The hybrid fuel cell design is a new concept which will require further development in order to increase its overall efficiency. Details of the design can be found in Appendix C.

ALWATT HYDROGEN GENERATOR

Hydrogen, of course, is the other requirement for the fuel cell to produce power. Although there are many possible sources of hydrogen, the next section will show that the Alwatt system provides a much safer and volumetrically superior option for the CFFC. The Alwatt is a corrosion cell where the aluminum is reacted with seawater to provide some electrical power and a significant amount of hydrogen as a by-product. This permits the use of the reactant in-situ to provide a source of gaseous hydrogen at ambient pressure.

The overall reaction is:

$$Al + 3H_2O \text{ ---> } Al(OH)_3 + \frac{3}{2} H_2$$

More details about the Alwatt system can be found in Appendix D.

The following are some salient features of the CFFC system designed to provide a power of 10 watts continuously for a duration of one year.

	Volume (liters)	Weight (kg)	Power Generated /Consumed (Watts)
Fuel Cell	2.2	3.33	+10.0
Gill	2.5	2.2	0
Alwatt	45.4	113.0	+2.30
Seawater Pump	*	*	-1.15
Carrier Pump + Control	*	*	-1.15
Total	50.1	118.53	+10.00

*Included in Alwatt volume and weight.

2.2 Design

2.2.1 System Energy Balance

The chemical reaction taking place in the Alwatt is as follows:

$$2\,Al + 6\,H_2O \text{ -----> } 2\,Al(OH)_3 + 3\,H_2$$

From this equation, we can derive the following:

2 moles of Aluminum give 3 moles of Hydrogen,
Or, 1 g. of Aluminum gives 1.2444 liters of Hydrogen.

From the Alupower report[1] on the performance of the Alwatt, we know that

1 g. of Aluminum gives 1.5 A-hrs. at 0.25 V,
1 g. of Aluminum gives 0.25 X 1.5 = 0.375 W-hrs of energy.
Therefore, the energy density of the Alwatt is 0.375 W-hrs/g or 375 W-hrs/kg. of aluminum

To calculate the energy derived from the Hydrogen evolved by the Alwatt,

1 mole of Hydrogen gives 2 X 96,500 C or A-sec, (2 electrons/molecule of H_2),
1 mole of Hydrogen gives 193,000 A-sec or 53.6111 A-hrs,
1 l of Hydrogen gives 2.3934 A-hrs, (since 1 mole = 22.4 liters), and
1 g. of Aluminum gives 2.9784 A-hrs (since 1 g of Aluminum = 1.2444 l of H_2).

If the Hydrogen can be oxidized in a fuel cell at a potential of 0.6 V (which is half the theoretical voltage that can be obtained from that process), we can derive the following:

1 g. of Aluminum gives 2.9784 A-hrs X 0.6 V = 1.787 W-hrs of energy via H_2,
The energy density of the Hydrogen fuel cell is 1.787 W-hrs/g or 1787 W-hrs/kg of Aluminum.

[1] B.M.L. Rao, W. Halliop, Alupower Report on Hydrogen and Contaminant Study, submitted to Aquanautics, Reported to DARPA, Quarterly Report of Oct. '89 - Dec. '89.

When the two systems are superimposed, the energy density is 2162 W-hrs/kg of Aluminum, which is roughly a factor of 5.75 higher than the energy density of the Aluminum alone in the Alwatt, where the Hydrogen by-product is wasted.

The above calculations are based on a unit quantity of aluminum and do not relate to system volume or weight. The assumptions were:

1) For Alwatt:

Operating Voltage	=	0.25 V
A-hr./g of Al	=	1.5 (theoretical 3)

These above numbers were taken from Alupower report, Alupower being manufacturer of the Alwatt system.

2) For Aquanautics CFFC System:

Fuel Cell Voltage	=	0.6
Hydrogen Utilization	=	60%

The fuel cell voltage constitutes a performance target, which will be discussed later. But utilizing the full amount of hydrogen generated in Alwatt is virtually impossible. The major loss will be:

1) Through the fuel cell membrane by diffusion
2) In the seawater flowing through Alwatt by dissolution

The magnitudes of these losses are calculated in Section 3.1.

From these calculations we can conclude that the amount of H_2 needed/watt assuming a fuel cell voltage of 0.6V) is:

1)	For fuel cell reaction	=	11.6 ml/min
2)	For loss through fuel cell	=	5 ml/min
3)	For loss through seawater through Alwatt	=	1.7 ml/min
	TOTAL	=	18.3 ml/min
	Aluminum needed	=	14.7 mg/min

From the Alupower report, it was determined that the Alwatt at 6000 m will have a starting voltage of around 0.22 volts. However, at 0.22 volts and 0.15 A-hr/g of Al, 14.7 mg/min will generate around 290 mW. Since the voltage will drop as Al gets consumed and due to shunt current losses, a further 20% drop was assumed, leading to 230 mW.

2.2.2 Aquanautics System Comparison With Lithium Thionyl Chloride Battery

In the preceding section, various types of oxygen sources, hydrogen sources, and energy sources have been evaluated. In each case, the technology offering the smallest size has been selected and the Aquanautics CFFC system defined as an integration of these best options. This section deals with the evaluation and sizing of the integrated system and its comparison with systems based on competing technologies.

The size of the Aquanautics CFFC system was calculated by first computing individual component size. The equations and theory behind the sizing of individual components are discussed in the succeeding subsections.

Table 2.1 shows a summary spreadsheet indicating all the important parameter values of the system for a 10W, 1 year system.

2.2.3 Calculation of the Gill Volume and Weight

The gill volume and weight were calculated on the basis of the following two equations that were derived to describe the seawater pumping power and the oxygen flux through the gill:

$$\frac{P\,V^2}{Q^3\,l^2\,\rho} = 13.5093\,\frac{\xi^{3.4}}{(\xi-1)^{3.2}}\left[\frac{\upsilon}{D}\right]\left[\frac{V\,D}{Q\,l^2}\right]^{0.2}\left[\ln\frac{C_{si}}{C_{si}-\frac{N}{Q}}\right]^{1.2} \qquad (2.2.1)$$

$$\ln\left\{\frac{C_{si}}{C_{si}-\frac{N}{Q}}\right\} = 4.3354\left[\frac{D^2\,V^2\,l}{\xi\,(\xi-1)^2\,Q^2\,d_o^5}\right]^{(1/3)} \qquad (2.2.2)$$

where,

P is the theoretical power needed for seawater pumping (W),
V is the volume of the gill fiber bed (m^3),
Q is the seawater flow rate through the gill (m^3/s),
l is the thickness of the gill fiber bed (m),
ρ is the density of the seawater (kg/m^3),
ξ is the fiber spacing factor, such that x d_o is the distance between the centers of adjacent fibers in one layer,
υ is the kinematic viscosity of seawater (m^2/s),
D is the diffusivity of oxygen through seawater (m^2/s),
C_{si} is the initial concentration of oxygen in seawater (std m^3/m^3),
N is the oxygen flux desired for the system (std m^3/s), and
d_o is the outer diameter of the gill fibers (m).

The derivation of these two governing equations is shown in Section 4.

The net power output of the system was used to specify the value for the seawater pumping power P in Equation 2.2.1. For example if the net power was assumed to be 10 W, for a system of that size, it was determined that the Alwatt would produce 2.3 W. Based on the assumption that the Alwatt power would be used for the various hotel loads, 1.15 W or 50% of the Alwatt output was set aside for seawater pumping. A seawater pumping efficiency of 10% was assumed and the theoretical value of the pumping power P was assumed to be 0.115 W. The oxygen flux desired was calculated from the net output power, which was assumed to be supplied by the Hydrogen-Carrier fuel cell. The net output voltage of the fuel cell was assumed and the cell current calculated from the equation,

$$I = \frac{P_n}{E} \qquad (2.2.3)$$

where, P_n is the net power output (W), and
E is the cell potential (V).

The oxygen flux needed was calculated from the current value obtained from Equation 2.2.3 by using the following equation:

$$N = \frac{I}{n F} \qquad (2.2.4)$$

where, n is the electron count (4 electrons/molecule of oxygen),
F is the Faraday Constant (96,500 C/mole), and
N is the oxygen flux (mol/s).

Table 2.1

19-Jul-89

Model of Direct Feed Fuel Cell and Gill
With Carrier Directly Reduced at the Fuel Cell Cathode

Inputs

Sym	Units	
1000 W	W	Net Power
1.08 Eo	v	Fuel Cell E0
0.48 Ep	v	Losses in Fuel Cell Efficiency
300 i	A/m^2	Fuel Cell Current Density
25 Rf	1/m	Fuel Cell Packing Density
1 L	year	Endurance
1500 rho_c	kg/m^3	Density of the fuel cell
2500 rho_a	kg/m^3	Density of Alwatt Cell

Outputs

	Units	
5.56E+00 Af	m^2	Fuel Cell Area
4.96E-02 Qs	m^3/s	Seawater Flow Rate
0.60 E	volts	Fuel Cell Voltage
2.22E-01 Vf	m^3	Fuel Cell Volume
1.67E-01 Vg	m^3	Theoretical Gill Volume
50% ng		Gill volume overhead allowance
2.50E-01 Vga	m^3	Actual Gill Volume
4.72E-01 Vfg	m^3	Gill Volume + Fuel Cell Volume
1.82E+00 Vh	m^3	Theoretical Hydrogen Source (Alwatt) Volume
40% nh		Packing efficiency + H2 generation efficiency of Alwatt
4.54E+00 Vha	m^3	Actual volume of Hydrogen source (Alwatt)
5.01E+00 Vt	m^3	Total Volume
2.21E+02 Wg	kg	Gill Weight
1.13E+04 Wa	kg	Alwatt Weight
3.33E+02 Wc	kg	Fuel Cell Weight
1.19E+04 Wt	kg	Total Weight

Calculations

	Units	
1666.67 If	amp	Fuel Cell Current
9.67E-05 Qo	m^3/s	Oxygen Consumption rate
1.93E-04 Qh	m^3/s	Hydrogen consumption rate
8.40E-02 P/w_den	W/kg	Gravimetric Power density
2.00E+02 P/v_den	W/m^3	Volumetric Power density
7.36E+02 E/w_den	W-hr./kg	Gravimetric Energy density
1.75E+06 E/v_den	W-hr./m^3	Volumetric Energy density

Gill V & Q= f(P)

Inputs		
P	11.5	W
L	0.025	m
rho	1025.8	kg/m^3
z	4	
u	1.7621E-06	m^2/s
D	2.1E-09	m^2/s
Cs	0.003	m^3/m^3
N	9.6718E-05	m^3/s
do	0.0003	m

Lumped Variables	
w,a	17.9372197
x,b	3019.45049
y,c	0.46829456
A	0.03223949
B	7.78125408

Outputs		
V	0.16654814	m^3
Q	0.04958748	m^3/s

Q	f of Q	fp of q	Qp	expBQ^(2/3)	Q2thirds
0.04958748	7.7139E-13	2.55857433	0.04958748	2.85839971	0.13497335

Gill Volume and Weight

Conversion of Gill Volume to Weight

Input Parameters

di	0.00025	m
do	0.0003	m
V	0.16654814	m^3
den_o	2200	kg/m^3
den_f	1200	kg/m^3
den_c	1140	kg/m^3
zeta	4	

Calculations

Vo	0.08327407	m^3
Vf	0.00999219	m^3
Vc	0.02270953	m^3

Output Gill Weight

W	221.082461	kg.

A spreadsheet, "Gill V & Q = f(P)," was used to compute the gill volume V and seawater flow rate Q from Equations 2.2.1 and 2.2.2 using the Newton-Raphson method. Once the gill volume V was calculated another spreadsheet, "Gill Volume and Weight," was used to compute the weight of the gill. The gill volume V obtained from Equations 2.2.1 and 2.2.2 represent only the volume of the fiber bed. This value of V was multiplied by a factor of 1.5 to obtain a total gill volume including the support structures and the seawater pump. Therefore, the gill packaging efficiency was assumed to be 67%. The overall gill weight was now assumed to consist of three essential components as shown in Equation 2.3.5.

$$W_g = W_o + W_f + W_c \tag{2.2.5}$$

where, W_g is the total weight of the gill (kg),
W_o is the weight of the gill support structure and pump (kg),
W_f is the weight of the gill fibers (kg), and
W_c is the weight of the carrier in the gill (kg).

The weights of the individual gill components were obtained by simply multiplying the volumes associated with those components by a density. The gill support structure volume was, as mentioned before, 0.5 V. The fiber volume and carrier volume were computed to be,

$$V_f = \frac{p\,V}{4\,\xi}\left\{1 - \frac{d_i^2}{d_o^2}\right\} \tag{2.2.6}$$

$$V_c = \frac{p\,V\,d_i^2}{4\,\xi\,d_o^2} \tag{2.2.7}$$

where, V_f is the volume occupied by the fibers (m^3),
V_c is the volume occupied by the carrier in the fibers (m^3), and
d_i is the inner diameter of the fibers (m).

The densities that were assumed for the various components are as follows:

ρ_o = 2200 kg/m^3 (gill packaging and pump),
ρ_f = 1200 kg/m^3 (gill fiber material, polypropylene or polyethylene), and
ρ_c = 1140 kg/m^3 (carrier).

The weight of the gill was therefore calculated from the equation,

$$W_g = V_c\rho_c + V_f\rho_f + V_o\rho_o \tag{2.2.8}$$

2.2.4 Calculation of Fuel Cell Volume and Weight

The fuel cell volume and weight were calculated on the basis of the expected performance characteristics. The current calculated from Equation 2.2.3 was used to size the fuel cell. The current density was assumed to be 30 mA/cm^2 or 300 A/m^2. Current densities two orders of magnitude higher than this have been achieved in conventional fuel cells using Hydrogen and Oxygen and therefore, 30 mA/cm^2 represents a rather conservative estimate. This current density was divided into the total cell current to yield the cell area as follows:

$$A_C = \frac{I}{i} \qquad (2.2.9)$$

where, A_C is the area of the fuel cell membrane (m^2),
I is the fuel cell current (A), and
i is the current density (A/m^2).

The fuel cell packaging efficiency was calculated to be 25 m^2/m^3 of volume. This indicates that one cubic meter of fuel cell volume was assumed to hold 25 m^2 of membrane area. This number corresponds to the packing efficiency of the multipurpose ABC-250 cell that has been developed at Aquanautics for its oxygen extraction system. The same cell can be employed as a fuel cell by incorporating the appropriate electrode configuration and by using the fuel cell membrane.

Therefore the volume of the fuel cell V_{fc} was calculated using Equation 2.2.2.

$$V_{fc} = \frac{A_C}{25} \qquad (2.2.10)$$

From the ABC-250 experience, it is known that the cell density, which is a composite of that of the cell parts, is about 1500 kg/m^3. The same number was used for the purposes of sizing the fuel cell also, given the adaptability of the ABC-250 design. This number is conservative given the fact that a regular electrochemical cell has liquid electrolyte in both chambers (anode and cathode) while the fuel cell application would entail use of liquid electrolyte - carrier in this case - only in the cathode chamber. Multiplying the fuel cell volume V_{fc} by the cell density yielded the cell weight W_{fc} as shown in Equation 2.2.11,

$$W_{fc} = 1500\, V_{fc} \qquad (2.2.11)$$

2.2.5 Calculation of the Alwatt Volume and Weight

Of the three major components of the Aquanautics system for oxygen extraction and power generation, the Alwatt is the only one whose size depends on the endurance of the system. The Alwatt system was sized based on the quantity of Hydrogen needed to produce the required W-hrs of energy. The capacity of the system was calculated from Equation 2.2.12.

$$C = \frac{P_n\, T}{E} \qquad (2.2.12)$$

where, C is the capacity of the system (A-hrs),
T is the system endurance (hrs),
P_n is the net power output of the system (W), and
E is the cell potential of an individual fuel cell (V).

The amount of Hydrogen required over the lifetime of the system was calculated from the current capacity of the system as follows:

$$Q_h = \frac{3600\ C}{n\ F} \qquad (2.2.13)$$

where, Q_h is the quantity of Hydrogen storage required (moles)
n is the electron count for Hydrogen (2 electrons/molecule H_2), and
F is the Faraday Constant (96,500 C/mole).

The equation for the reaction taking place in the Alwatt is as follows:

$$2\,Al + 6\,H_2O \text{ -----> } 2\,Al(OH)_3 + 3\,H_2.$$

From this chemical reaction, it is obvious that to produce 1 mole of Hydrogen, 2/3 moles or 18 g. of Aluminum are required. Therefore the quantity of Aluminum required to store Q_h moles of Hydrogen is calculated by multiplying Q_h into 18. The Alwatt volume could then be calculated by using a density for the Aluminum of 2800 kg/m^3. In addition, a few other factors had to be taken into account to compute the Alwatt volume. They were:

1) Loss of Hydrogen through diffusion and dissolution in seawater,
2) Packaging inefficiencies in the Alwatt cell, and
3) Support structures for the Alwatt.

Accordingly the theoretical volume for the Alwatt derived in the preceding paragraph was multiplied by a factor of 2.5 to account for the above contingencies and the final Alwatt volume obtained. A density of 2500 kg/m^3 was attributed to the Alwatt and the weight calculated by multiplying this density into the volume of the Alwatt. The density of the Alwatt is lower than the density of the Aluminum itself, because of voids between plates of Aluminum fuel and the fact that the packaging material into which the Alwatt is built is likely to be non-metallic and made of plastic material.

The volume of the carrier pump and the controls were not included in this analysis, and they are expected to be negligible when compared to the size of the three major components analyzed here. Moreover, some of the packaging efficiencies assumed in this study are generous enough that they could be assumed to include allowances for the carrier pump and control electronics, if any. For example, the volume of the carrier pump, for such a system, from laboratory experience is not likely to be more than 0.75 liters. The carrier pump will be pumping anywhere between 200 and 600 ml/min of carrier fluid through the system at current performance levels and pumps to do this are available commercially in small packages. It is therefore assumed that employing conservative packaging efficiencies for the three major components would provide enough contingency for the carrier pump and system controls. This is not expected to lead to significant errors.

2.2.6 Calculation of Competing System Sizes

The sizes of competing systems were calculated based on published energy densities. The specifications of most power systems include data on the gravimetric and volumetric energy density and this data was used in the following equations to determine the system weight and volume:

$$W_s = \frac{P_n\ T}{e_{sg}} \qquad (2.2.14)$$

$$V_S = \frac{P_n T}{e_{sv}} \qquad (2.2.15)$$

where, W_S is the weight of the competing system (kg),
V_S is the volume of the competing system (m^3),
P_n is the power output of the system (W),
T is the endurance of the system (hr)
e_{sg} is the gravimetric energy density of the system (W hr/kg), and
e_{sv} is the volumetric energy density of the system (W hr/m^3).

Implementation of System Sizing Model

The sizing model discussed in the above subsections was implemented in spreadsheets. The gill sizing was accomplished by solving Equations 2.2.1 and 2.2.2 iteratively by using the Newton-Raphson method. To do this, the two equations were combined to yield an equation of the form,

$$f(Q) = B\,Q^{(2/3)} + \ln\left(1 - \frac{A}{Q}\right) = 0 \qquad (2.2.16)$$

where, A and B are constants which combine the parameters D, u, r, C_{si}, N, P, ξ, d_o, and l,
Q is the seawater flow rate.

Equation 2.2.16 was then solved using the Newton-Raphson method and the gill volume determined by substituting the value of Q, thus determined, into Equation 2.2.2. The iterative process was implemented in a spreadsheet called "Gill V & Q = f(P)" and the output namely the values of V and Q were used by the other linked spreadsheets. The gill volume was converted into a gill weight by the spreadsheet "Gill Volume and Weight", while the volume and weight of the fuel cell and the Alwatt were computed in the main spreadsheet called "Deep Power Model". The main spreadsheet also served as the point at which the assumptions to the model were introduced and the results of the model supplied to tables for tabulation of the system size as a function of endurance or fuel cell voltage.

The equations describing the size of competing systems were implemented in the main spreadsheet "Deep Power Model" also. This was done so that the tables used for plotting would have the sizes of both the Aquanautics CFFC as well as the alternatives. Printouts of the spreadsheets are attached for reference.

3.0 FUEL CELL

3.1 Calculation of Hydrogen Leak Through Fuel Cell and Seawater Flow Through Alwatt System

3.1.0 Background

The DARPA project calls for a study into the feasibility of extracting oxygen from seawater and combining this oxygen with hydrogen in a fuel cell to produce electrical power. The hydrogen is generated from an aluminum-seawater cell as a by-product. The system is being considered for application at depths of up to 6000 m under the ocean and is being designed to operate at the ambient pressure. This implies that the hydrogen in the fuel cell would be at pressures of up to 600 atmospheres. The high hydrogen pressure in the fuel cell creates a problem, namely one of diffusion to the sea through the fuel cell membrane, carrier and gill membrane to the seawater. Normally, since the atmosphere does not contain significant quantities of hydrogen, the hydrogen content of seawater can be considered to be zero. This causes existence of a steep hydrogen concentration difference between the fuel cell anode and the seawater surrounding the system. Since the carrier and the seawater come in contact with one another through the gill, there is a potential for hydrogen diffusion through the gill to the ocean. This diffusive flux has to be estimated so that appropriate measures can be enacted to minimize the loss of hydrogen to the seawater.

3.2.0 Objective

The objective of this study is to determine the rate of hydrogen diffusion from the fuel cell to the seawater. This is to be accomplished by considering the hydrogen permeability of the fuel cell membrane as well as the mass transport coefficients for the carrier and seawater streams. Another objective of this exercise is to set up a model for the diffusion of hydrogen through the system so that remedial measures can be identified. Also such a model is expected to help identify the system component that controls the flux of hydrogen through the system.

3.3.0 Model for Hydrogen Transport

3.3.1 Overall Transport Equation

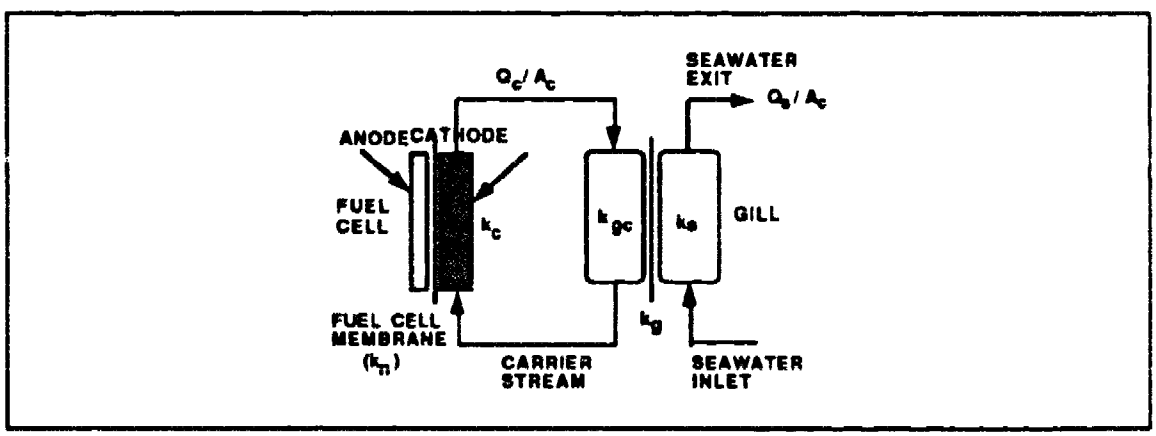

Figure 3.3.1 Diffusion Path for Hydrogen from Fuel Cell to Seawater

The system schematic shown in Figure 3.3.1 identifies the various components of the mass transfer coefficient for hydrogen flux from the fuel cell to seawater.

The hydrogen transport problem can be modelled using an electrical analog with resistors in series. The effective mass transport coefficient for hydrogen flux from the fuel cell to the seawater can therefore be defined by Equation 3.3.1 which is normalized with respect to the area of the fuel cell membrane.

$$\frac{1}{k_e} = \frac{1}{k_{np}} + \frac{1}{k_{cp}} + \frac{A_c}{A_{gi} k_{gc}} + \frac{A_c}{Q_c} + \frac{A_c}{A_g k_s} + \frac{A_c}{Q_s} + \frac{A_c}{A_g k_g} \qquad (3.3.1)$$

where,

k_e is the effective mass transport coefficient for hydrogen transport from the fuel cell to the seawater (m/s),
k_n is the hydrogen permeability of the membrane (m/s),
p is the fraction of the total membrane area exposed by the fuel cell anode,
A_c is the area of the membrane in the fuel cell (m^2),
k_c is the mass transport coefficient for the carrier in the cathode of the fuel cell (m/s),
k_{gc} is the mass transport coefficient for the carrier stream in the gill (m/s),
A_{gi} is the surface area presented to the carrier by the inner surfaces of the gill hollow fibers (m^2),
k_s is the mass transport coefficient for the seawater stream flowing through the gill (m/s),
A_g is the area presented to the seawater by the outside surface of the gill hollow fibers (m^2),
k_g is the hydrogen permeability of the gill membrane (m/s),
Q_c is the flow rate of the carrier through the system (m^3/s), and
Q_s is the flow rate of seawater through the gill (m^3/s).

The permeabilities of the fuel cell membrane, k_c, and the gill membrane, k_g, are usually specified in terms of a flux rate per unit area per unit partial pressure difference (mol/s/m^2/atm). This can be converted to the standard mass transfer coefficient units of m/s by using Henry's Law. The solubility of hydrogen (given in mol/m^3/atm) can be divided into the published permeability to yield the familiar units of m/s. What is happening here is that hydrogen is diffusing from a gaseous phase to a dissolved phase where the solvent is a liquid. This means that the concentrations are usually expressed in two different units, atm for the gas phase and mol/m^3 for the dissolved state. Using Henry's Law allows conversion of the membrane permeability referred in terms of gas phase concentrations (atm) to liquid solution phase concentrations (mol/m^3).

Another point to be noted with respect to Equation 3.3.1 is that the overall mass transport coefficient is being referred in terms of the fuel cell membrane area. This is because the fuel cell membrane was determined to be the crucial and controlling component of the hydrogen diffusion problem. Therefore, optimization of the system will proceed by adjusting the fuel cell area and analyzing its implications.

The magnitude of the hydrogen transport can be gaged from the value of the term k_e, and the relative importance of its various constituents determined from the values of the individual components in Equation 3.3.1. The hydrogen transport can now be characterized by the equation,

$$Q_h = k_e A_c \Delta C, \quad (3.3.2)$$

where, Q_h is the flux rate of hydrogen (mol/s or m^3 @ STP/s), and
ΔC is the difference in hydrogen concentration between the fuel cell anode and the seawater (mol/m^3 or m^3 @ STP/m^3).

For the sake of clarity, moles are used as the preferred units for expressing hydrogen flux. Since the expression for k_e had been referred to the fuel cell area in Equation 3.3.1, use of A_c in Equation 3.3.2 is permitted. It can therefore be seen from Equation 3.3.2 that in order to reduce the magnitude of Q_h, the value of A_c has to be reduced. Since the units for k_e are m/s, the units for ΔC should be mol/m^3. The concentration of hydrogen in the gas phase at the fuel cell anode (given in atmospheres of pressure) will, therefore have to be converted to solution concentrations (mol/m^3) by using Henry's Law. The fuel cell anode hydrogen partial pressure is thus converted into a solution concentration that would exist in equilibrium with that partial pressure.

3.3.2 Determination of Fuel Cell Area

The fuel cell area is the most crucial component of the hydrogen diffusion problem. The area of the fuel cell membrane is determined from the current density that is found to be ideal for operation. The current density at the operating point is determined from the output power requirements and the cell voltage at that current density. The cell voltage is generally of the form,

$$V_c = V_o - \alpha i, \quad (3.3.3)$$

where, V_c is the fuel cell voltage under load (V),
V_o is the fuel cell voltage under no load conditions (V),
i is the current density (A/m^2), and
α is a constant (Ω - m^2).

The value of the constant a is dependent on a number of factors, such as mass transfer, activation kinetics and the cell impedance. One component of the cell impedance is the resistance of the membrane. This resistance is linearly dependent on the thickness of the membrane and therefore this can be easily incorporated into Equation 3.3.3 to give,

$$V_c = V_o - (\beta + t\, r_m)\, i, \quad (3.3.4)$$

where, β is a constant (Ω - m^2),
t is the membrane thickness (m), and
r_m is the specific resistance of the membrane (Ω - m^2/m).

This equation is derived by splitting the constant α from Equation 3.3.3 into two components, one related to the membrane resistance and the other encompassing the remaining components of the fuel cell losses. This helps to identify another parameter that affects Hydrogen diffusion, namely the thickness of the fuel cell membrane.

If the desired output power can be denoted by P, the cell area can be calculated from the equation relating cell voltage and current to power,

$$A_C = \frac{P}{V_C\, i} \tag{3.3.5}$$

where, P is the gross power output of the fuel cell (W), and
A_C is the fuel cell area (m^2).

At this stage, it is necessary to divide the total cell area into a number of individual cells to enable determination of the mass transport coefficient on the carrier side of the cell or in its cathode compartment. Usually the cell dimensions are restricted by designs that are commercially available, and it can be assumed here that the available cells have a length of l and a breadth of b. Therefore area of each individual cell is given by,

$$a_C = b\,l \tag{3.3.6}$$

where, a_C is the area of the individual cell (m^2),
b is the breadth of the cell (m), and
l is the length of the cell in the direction of carrier flow (m).

The number of cells is therefore given by

$$n_C = \frac{A_C}{a_C} \tag{3.3.7}$$

where, n_C is the number of cells

3.1.3.3 Membrane Permeability

The membrane permeability can now be calculated given the membrane thickness t. Manufacturers of membranes that are commonly used in fuel cells publish permeabilities for membranes of unit thickness. An example would be the units used to specify the hydrogen permeability of Nafion which is given in mol-mil/s/m^2/atm. The actual permeability of the membrane can be determined from this value, as well as its thickness and the solubility of Hydrogen in the liquid medium to which the transport is occurring. This yields,

$$k_n = \frac{K_n}{S_h\, t} \tag{3.3.8}$$

where, K_n is the specific permeability of the cell membrane (mol-mil /s /m^2/atm), and
S_h is the solubility of hydrogen in seawater (mol/m^3/atm).

3.3.4 Carrier Flow Rate

The carrier flow rate determines two constituents of the total hydrogen flux, namely diffusion on the cathode side of the fuel cell membrane and the capacity for transmission through the carrier itself. To determine the carrier flow rate, it is necessary to consider the hydrogen and oxygen consumption rates. The hydrogen consumption rate is directly dependent on the fuel cell current and is given by the equation

$$Q_{hc} = \frac{i A_c}{n F} \qquad (3.3.9)$$

where, Q_{hc} is the rate at which hydrogen is consumed in the fuel cell (mol/s),
n is the number of electrons involved in the oxidation of each hydrogen molecule (2). and
F is the Faraday constant (96,500 C/mol).

The hydrogen consumption rate yields the oxygen consumption rate by stoichiometry,

$$Q_{oc} = 0.5\ Q_{hc}, \qquad (3.3.10)$$

where, Q_{oc} is the rate at which oxygen is consumed (mol/s).

The carrier flow rate is also dependent on the fractional conversion of carrier in the fuel cell and the concentration of carrier in solution. The fractional conversion is a term that defines the proportion of carrier that is deoxygenated in the fuel cell. Hence,

$$Q_c = \frac{2Q_{oc}}{M_c f_c} \qquad (3.3.11)$$

where, Q_c is the carrier flow rate (m^3/s),
M_c is the molar concentration of the carrier solution (mol/m^3), and
f_c is the fractional conversion of the carrier in the fuel cell.

The use of the multiplier 2 in Equation 3.3.11 is indicative of the fact that the carrier is dimeric, namely that it takes two molecules of the carrier to bind one oxygen molecule. To calculate the mass transfer coefficient on the carrier side of the cell, the flow rate of carrier through each cell is calculated as per the equation,

$$q_c = \frac{Q_c}{n_c} \qquad (3.3.12)$$

where, q_c is the flow rate of carrier per cell (m^3/s).

3.3.5 Mass Transport of Hydrogen to the Carrier

The mass transport coefficient for the transport of hydrogen to the carrier in the cathode compartment of the fuel cell can be calculated based on the Leveque correlation for mass transport into flow in conduits. This correlation is expressed as:

$$Sh = 1.62\ Re^{0.33}\ Sc^{0.33} \left(\frac{df}{l}\right)^{0.33}$$

where, Sh is the Sherwood Number,
Re is the Reynolds Number,
Sc is the Schmidt Number,
d_f is the hydraulic diameter of the cathode conduit (m), and
l is the length of the flow path in the cathode compartment (m).

The equation describing the transport of hydrogen to the carrier in the fuel cell cathode compartment does not account for the likely presence of a high surface area electrode in that compartment. The presence of such an electrode, which may take on the form of a carbon felt, will serve to increase the resistance to hydrogen flux. The equation listed above, therefore, represents a worst case scenario. The dimensionless numbers referred to above are defined below.

$$Re = \frac{r_c\ q_c\ d_f}{\mu_c\ b\ t_f}$$

where, t_f is the thickness of the cathode compartment (m),
r_c is the density of the carrier (kg/m^3), and
m_c is the dynamic viscosity of the carrier ($N\ s/m^2$).

$$Sc = \frac{\mu_c}{r_c\ D_c}$$

where, D_c is the diffusivity of hydrogen in carrier (m^2/s).

$$Sh = \frac{k_c\ d_f}{D_c}$$

where, k_c is the mass transport coefficient for the carrier side of the cell (m/s).

The hydraulic diameter of the conduit d_f is defined in traditional terms as four times the cross-sectional area divided by the perimeter, and is therefore represented by,

$$d_f = \frac{4\ b\ t_f}{(b+t_f)}$$

Using the above equations, the carrier side mass transport coefficient was determined to be

$$k_c = 1.62 \left(\frac{q_c\ d_f\ r_c}{\mu_c\ b\ t_f}\right)^{0.33} \left(\frac{\mu_c}{\rho_c D_c}\right)^{0.33} \left(\frac{d_f}{l}\right)^{0.33} \left(\frac{D_c}{d_f}\right) \qquad (3.3.13)$$

3.3.6 Gill Sizing

Gill sizing is important to the hydrogen diffusion problem because hydrogen exits the system through the gill. It is, however, not likely that the gill will control the hydrogen flux because of its large interfacial area. It is likely not to provide significant resistance to hydrogen transport. The gill resistance to hydrogen transport is composed of three components just as in the case of oxygen transport into the system. These three components are the carrier side boundary layer, the membrane permeability and the seawater side boundary layer. To calculate the effects of the gill operation on the hydrogen flux, it is necessary to size the gill first. The gill sizing is dependent on the oxygen flux that is desired for system power generation. The gill design equations yield, the volume of the gill V_g, the area of the gill A_g, and the length of the fibers a. Also as a result of gill sizing, the flow rate of seawater can be calculated given the extraction efficiency of the system. The gill design also yields a thickness for the gill which is denoted here by l_g. The length of the fibers in a gill of square cross-section can be determined by the equation,

$$a = \left(\frac{V_g}{l_g}\right)^{0.5} \tag{3.3.14}$$

where, V_g, l_g and a are defined above.

The number of fibers, which is important in determining the flow and transport characteristics through each fiber, can be calculated from the surface area of the gill and the outer diameter of each fiber.

$$n_f = \frac{A_g}{\pi\, d_o\, a} \tag{3.3.15}$$

where, n_f is the number of gill fibers, and
d_o is the outer diameter of the gill fibers (m).

The flow rate of carrier through each gill fiber can therefore be calculated using the equation,

$$q_{cf} = \frac{Q_c}{n_f} \tag{3.3.16}$$

where, q_{cf} is the carrier flow rate through each fiber (m^3/s).

3.3.7 Mass Transport Coefficients in the Gill

The mass transport characteristics for hydrogen diffusion through the gill are determined using the correlations of non-dimensional numbers that have been derived for various flow situations and geometries. For the flow of carrier through the fibers, the Leveque correlation shown in the beginning of Section 3.3.5 is employed. This gives an expression for the mass transport coefficient shown below

$$k_{gc} = 1.62\left(\frac{4 q_{cf}\, \rho_c}{\pi\, d_i\, \mu_c}\right)^{0.33} \left(\frac{\mu_c}{\rho_c D_c}\right)^{0.33} \left(\frac{d_i}{a}\right)^{0.33} \left(\frac{D_c}{d_i}\right) \tag{3.3.17}$$

where, k_{gc} is the mass transport coefficient for the carrier side in the gill (m/s),
d_i is the inner diameter of the gill hollow fiber (m), and
q_{cf}, D_c, μ_c, ρ_c, and a have all been defined in Sections 3.3.5 and E.3.7.

For the hydrogen flux characteristics on the seawater side, a correlation derived by Yang and Cussler is used. This correlation was derived for flow perpendicular to a hollow fiber bed. This correlation relates the Reynolds, Schmidt and Sherwood numbers in the familiar fashion,

$$Sh = 1.38\, Re^{0.34}\, Sc^{0.33}.$$

Using the usual definitions of the above dimensionless numbers, the seawater side mass transfer coefficient is derived to be

$$k_S = 1.38\left(\frac{u_S d_O \rho_S}{\mu_S}\right)^{0.34}\left(\frac{\mu_S}{\rho_S D_S}\right)^{0.33}\left(\frac{D_S}{d_O}\right) \qquad (3.3.18)$$

where, u_S is the seawater velocity through the gill (m/s),
ρ_S is the seawater density (kg/m^3),
μ_S is the dynamic viscosity of the seawater (N s/m^2),
D_S is the diffusivity of hydrogen through seawater (m^2/s),
k_S is the mass transfer coefficient for hydrogen diffusion on the seawater side (m/s), and
d_O is the outer diameter of the gill hollow fibers (m).

The seawater velocity term u_S has to be determined from the seawater flow rate, taking into account the fact that the entire gill cross-section (a x a) is not available for seawater flow. This term was derived for a gill consisting of fibers (ξ d_O) apart and arranged in layers where adjacent layers are perpendicular to each other. The seawater velocity is derived to be,

$$u_S = \frac{Q_S \xi^2}{(\xi-1)^2\, a^2} \qquad (3.3.19)$$

where, ξ is the spacing factor for the fibers in the plane perpendicular to the seawater flow direction, such that the center to center distance between adjacent fibers is ξ d_O.

The mass transfer coefficients thus determined can be entered into Equation 3.3.1 to determine the effective mass transfer coefficient and the hydrogen flux from the fuel cell to the seawater.

3.4.0 Application of the Model to a Case Study

The model developed based on the equations derived in Section 3.3.0 was implemented in a spreadsheet. This was done to examine the Hydrogen diffusion characteristics and evaluate the effect of various fuel cell operating parameters on the extent of the Hydrogen loss through the fuel cell membrane. The parametric analysis was performed by plotting the fraction of the total Hydrogen consumed, that was lost to diffusion at various depths.

3.4.1 Solubility of Hydrogen in Seawater

Initially, to examine the Hydrogen diffusion phenomenon, data was collected for the solubility of Hydrogen in seawater, since it is clear that the Hydrogen diffusion seeks to establish such an equilibrium. As part of the feasibility study undertaken by Alupower[2] the solubility of Hydrogen in seawater was calculated based on published data for Hydrogen solubility in pure water. The results of this study are summarized in Table 3.4.1. Included in Table 3.4.1 are the solubility of Hydrogen in seawater as a function of depth and a conversion of this solubility into a Henry's Law Constant. The Henry's Law Constant is usually defined in the equation,

$$p = H\chi \qquad (3.4.1)$$

where, p is the partial pressure of the gas under consideration (atm),
χ is the mole fraction of the gas dissolved in the solvent (moles solute/mole solution), and
H is the Henry's Law Constant (atm mole solution/mole solute).

It is obvious here that the Henry's Law Constant depicted in Table 3.4.1 is the reciprocal of the constant used in Equation 3.4.1. The constant in Table 3.4.1 has units that allow it to be used as the parameter S_h in Equation 3.3.8.

TABLE 3.4.1

DEPTH (m)	PRESSURE (atm)	SOLUBILITY (std m^3/m^3)	HENRY'S CONST (std $m^3/m^3/atm$)
0	1.0000	0.019	0.0190
500	50.6575	0.93	0.0184
1000	100.3151	1.855	0.0185
3000	298.9452	5.347	0.0179
5000	497.5753	8.569	0.0172
7000	696.2054	11.646	0.0167
10000	994.1506	15.679	0.0158

3.4.2 Assumptions in the Case Study

This section lists the main assumptions made in evaluating the Hydrogen diffusion problem. These assumptions are divided into appropriate sections dealing with individual components as below:

[2]Reference already cited.

1) Power System Assumptions:

System Power	=	1000 W
Parasitic Power Consumption (Pumps & Controls)	=	230 W
Seawater Pump Power Consumption	=	115 W

2) Fuel Cell Assumptions: (Data from Nafion Specification Sheet with Giner Electrode)

Fuel Cell Membrane Permeability (K_n)	=	520 cm^3-mil/(ft^2 hr atm)
Fuel Cell Membrane Porosity (p)	=	30%
Fuel Cell Sizing (ABC-250) (l X b)	=	10 cm X 25 cm
Fuel Cell Membrane Specific Resistance (r_m)	=	0.1463 $\Omega m^2/m$
Slope of Cell Potential - Current Density curve (β)	=	0.001148 $\Omega m^2/m$
Thickness of Fuel Cell Chamber (tf)	=	7.5 mm

3) Carrier Property Assumptions:

Diffusivity of Hydrogen through carrier (D_C)	=	5.36 X 10^{-9} m^2/s
Density of carrier (ρ_C)	=	1140 kg/m^3
Dynamic Viscosity of carrier (μ_C)	=	1.455 cP
Concentration of Carrier in Solution (M_C)	=	0.4 M or 400 $moles/m^3$

4) Gill Sizing Assumptions:

Gill Thickness (l_g)	=	0.05 m
Fiber Outer Diameter (d_o)	=	400 μm
Fiber Inner Diameter (d_i)	=	350 μm
Fiber Spacing Factor (ξ)	=	4

5) Seawater Property Assumptions:

Initial Oxygen Concentration in Seawater (C_{Si})	=	3 ml @ STP/l
Density of Seawater (ρ_S)	=	1025.8 kg/m^3
Kinematic Viscosity of Seawater (υ_S)	=	1.7621 X 10^{-6} m^2/s
Diffusivity of Oxygen through Seawater (D_{OS})	=	2.1 X 10^{-9} m^2/s
Diffusivity of Hydrogen through Seawater (D_S)	=	5.36 X 10^{-9} m^2/s

3.4.3 Parametric Variations in Case Study:

The parametric analysis was conducted, as mentioned earlier, to evaluate the fraction of Hydrogen consumption that is lost through diffusion to seawater at various depths. This analysis was conducted by varying the values of four parameters that were thought to impact the diffusion rate directly. These parameters are:

1) Fuel Cell Membrane Thickness (t),
2) Fuel Cell Current Density (i),
3) Fractional Conversion in the Fuel Cell (f_C), and
4) Open Circuit Cell Fuel Cell Potential (V_O).

Table 3.4.2 shows the values of the various parameters that were used in the parametric analysis. This table also depicts the baseline values used in the analysis. The baseline value represents the value of the parameter that was held constant while the variation of another parameter was being studied. For instance, in studying the effect of the membrane thickness by varying its value, the value of the current density was held constant at the baseline value, namely 30 mA/cm^2.

Table 3.4.2

Memb. Thick. (mils)	Current Density (mA/cm^2)	Fractional Conv (%)	OC Cell Poten. (V)	Comments
5.0	10	2.5	0.75	
7.5	20	10.0	0.85	
10.0	30	5.0	0.95	Baseline
12.5	40	15.0	1.05	
15.0	50	25.0	1.15	

3.4.4 Method of Application of Model

The model was applied to evaluate the different values of the mass transport coefficients in Equation 3.3.1. For the purposes of this analysis, it was assumed that the gill membrane permeability k_g did not control the Hydrogen mass transport and was therefore ignored. The other mass transport coefficients calculated included the following:

k_n Membrane Permeability
k_C Fuel Cell Cathode Mass Transfer Coefficient
k_{gc} Carrier Side Mass Transfer Coefficient for the gill
k_S Seawater Side Mass Transfer Coefficient for the gill
Q_C/A_C Carrier Capacity
Q_S/A_C Seawater Capacity

To perform these calculations, three inter-linked spreadsheets were devised. The first spreadsheet contained the information regarding the solubility of Hydrogen at various depths that is shown in Table 3.4.1. This table was used as a look-up sheet, and was referred to whenever information regarding Hydrogen dissolution equilibrium was needed. The second sheet was devoted to gill sizing. Since the Hydrogen diffusion is affected by gill sizing and the seawater flow rates, this information was considered necessary. The gill sizing spreadsheet was set up to receive the seawater pumping power information from the main sheet, which constituted the actual calculation of the hydrogen diffusion mass transport coefficients.

The power output of the system was entered through the main spreadsheet and an allotment for seawater pumping power calculated from the net power. This pumping power information was shared by the gill sizing spreadsheet, which used it along with the gill sizing and seawater property assumptions to calculated a gill size. The gill sizing

spreadsheet used the two simultaneous equations derived in Section 4. These equations were solved for the given power value to yield gill volume and the seawater flow rate. The gill sizing spreadsheet used the Newton-Raphson method to solve the gill design equations.

The gill sizing information and the seawater flow rate from the gill sizing spreadsheet were then used by the main spreadsheet to calculate the various mass transport coefficients as per the equations developed in Section 3.3.0.

3.5.0 Results and Discussion of the Parametric Analysis

As mentioned above, the effects of the various parameters are investigated by plotting the percentage of Hydrogen lost to diffusion as a function of depth. The effect of each parameter is investigated in a separate section.

3.5.1 Effect of Fuel Cell Membrane Thickness

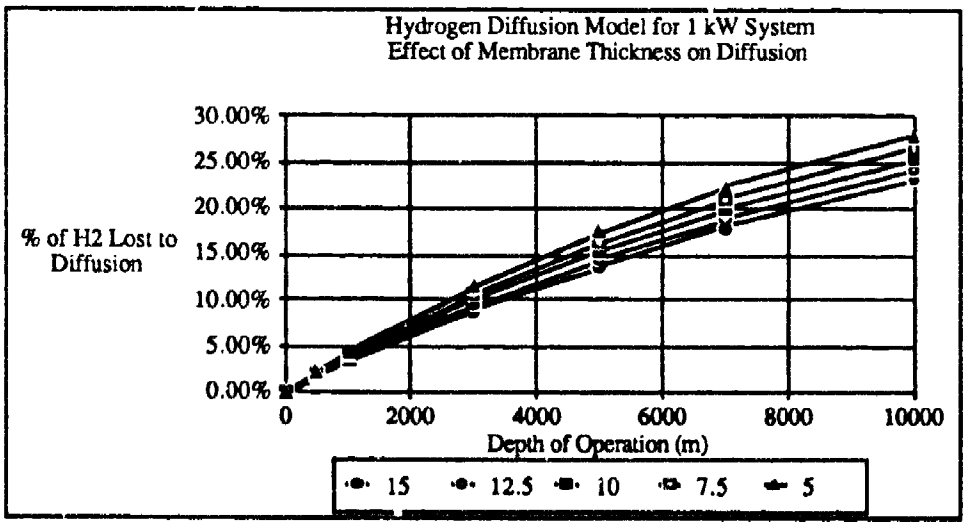

Figure 3.5.1 Hydrogen Diffusion for various Fuel Cell Membrane Thickness values

Figure 3.5.1 depicts the variation of Hydrogen loss due to diffusion as a function of depth for various values of the fuel cell membrane. The values in the legend of Figure 3.5.1 have units of mils (milli-inches). As expected, the diffusion loss is least for the thickest membranes and the increase of the diffusion rate as a function of depth is not linear. This is because the solubility curve for Hydrogen is not linear. A point to note here is that increased membrane thickness will cause an increase in the ohmic losses in the cell. This is due to the increased electrical resistance of thicker membranes. This drop in voltage would normally cause the need for higher currents to maintain the net power output. An increased current at constant current densities implies greater cell areas, which would in normal circumstances cause increased hydrogen diffusion. In the model however, the contribution of the term tr_m - which represents the resistance of the membrane - is smaller than that of b which represents other contributions to losses in the cell. The output voltage is hence not very highly sensitive to the membrane thickness. Therefore the negative effect of increased cell losses are more than offset by the beneficial impact of decrease in fuel cell membrane permeability.

3.5.2 Effect of Fuel Cell Current Density

Figure 3.5.2 depicts the variation of the diffusion loss of Hydrogen for various values of the current density (units in the legend are A/m^2) in the fuel cell. As expected the current density has a strong effect on the diffusion loss. This is because the area of the fuel cell is inversely proportional to the current density. Lower current densities therefore necessitate the use of larger fuel cell areas causing the potential for greater diffusion of Hydrogen. The increased diffusion rates at low current densities are slightly offset by the fact that fuel cell ohmic and kinetic losses are reduced at low current densities. Therefore the cell output voltage is increased and the fuel cell current needed to provide the necessary power decreases. This beneficial impact is, however, not very significant compared to the impact of the increased cell area as is evident from Figure 3.5.2.

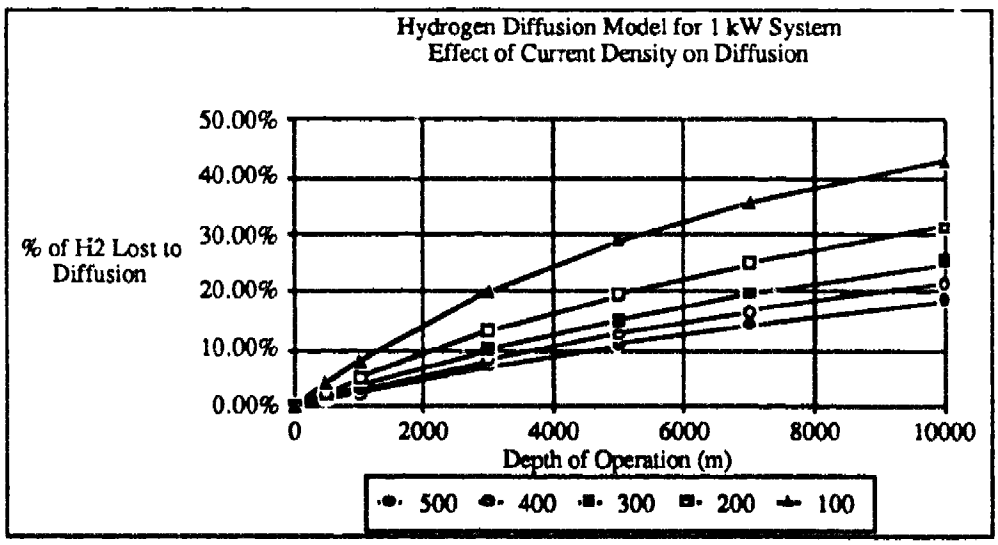

Figure 3.5.2 Hydrogen Diffusion for various Fuel Cell Current Density values

3.5.3 Effect of Fractional Conversion of Carrier in Fuel Cell

The fractional conversion is defined as that fraction of the total number of moles of carrier presented to the fuel cell that is converted. Conversion, here, refers to the electrochemical release of oxygen for purposes of producing power from the fuel cell. The concept of fractional conversion is normally tied into the current density, that is higher the current density, greater the number of carrier molecules being reduced, and hence greater the fractional conversion. For purposes of this analysis, the fractional conversion and the current density are treated separately to evaluate, numerically, the effect of each. In a working device, it is expected that the larger fractional conversions would be obtained at high current densities.

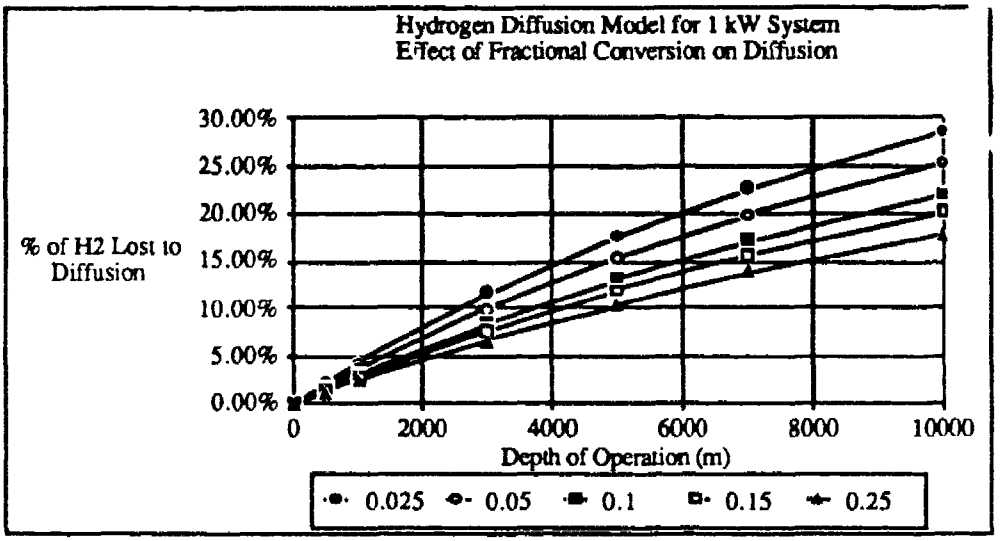

Figure 3.5.3 Hydrogen Diffusion for various Fractional Conversion values

Figure 3.5.3 depicts the variation of the Hydrogen diffusion with different values of the fractional conversion. As expected the Hydrogen loss decreases with increasing fractional conversion. This effect of higher fractional conversion is directly manifested in smaller carrier flow rates. This causes a decrease in the contribution of the carrier flow to the overall mass transport coefficient and therefore lower Hydrogen diffusion rates. When, as is expected in a real process, the increased fractional conversion is coupled with the higher current density, the decrease in Hydrogen diffusion will be more dramatic. This is because the beneficial effects of decreased carrier flow rate will be coupled with that of the lower fuel cell area.

3.6.0 Hydrogen Loss as Dissolved in Seawater through Alwatt System

Alwatt needs certain amount of seawater flow to prevent clogging of their system. This is quoted to be 0.2 A-hr./ml of electrolyte or seawater (Reference cited).

Calculation of hydrogen loss via seawater flow through Alwatt:

1 g of Al produces 1.2444 liters of H_2

1 g. of Al provides 1.5 A-hr.

ml of seawater/g of Al to prevent clogging:

$$\frac{1.5 \text{ A-hr/g of Al}}{0.2 \text{ A-hr/ml of electrolyte}} = 7.5 \text{ ml of seawater/g of Al}$$

Therefore, 1.2444 liters of H_2 ($\equiv$ 1 g of Al) would need 7.5 ml of seawater.

At 6000 m, H_2 solubility is 10 ml/ml of seawater (Reference cited).

Therefore, if we provide the minimum seawater flow of 7.5 ml of seawater/g of Al consumed, we would lose 75 ml of H_2 out of 1.24 liters produced. With a safety factor of 65%, the hydrogen loss will be 10%. So design point seawater flow is 12.4 ml/g of Al consumed.

The loss is very strongly dependent on the pressure or depth of operation. At 6000 m, the maximum loss is about 30% of total amount of hydrogen coming to fuel cell (see Figures 3.5.1 - 3.5.3, this appendix). Therefore, for each watt generated by fuel cell, we need:

1)	for electrochemical reaction: (1 l of $H_2 \equiv$ 2.39 A-hr)		11.6 ml/min
2)	for loss through fuel cell	$11.6 \times \frac{3}{7}$	5 ml/min
3)	for loss through seawater thru Alwatt	(11.6 + 5) x 0.1	1.7 ml/min
		Total H_2 need	18.26 ml/min

The development of a Hydrogen loss model was found to be important to the analysis of the whole deep submergence power system. The system analysis was performed to compare the energy density and performance of the Aquanautics system with those based on competing technologies. In order to size the Aquanautics system, it is necessary to determine the size of the Hydrogen source, the Alwatt battery in this case. To determine the size of the Alwatt, it is imperative the total required capacity of Hydrogen be computed, taking into account not only the amount that is likely to be consumed, but also that which is likely to be wasted in diffusive losses. This model helped in identifying the magnitude of the latter, and the former could be had from stoichiometry, leading in turn to an accurate and reliable estimate for the size of the Alwatt as well as the integrated Aquanautics deep submergence power system.

4.0 GILL: Gill Sizing vs. Seawater Pumping

4.0.0 Introduction

This study was performed as part of a project evaluating the feasibility of using oxygen dissolved in seawater to produce power under the sea. The power source being evaluated would use the extracted oxygen and hydrogen from another source for purposes of producing power in a fuel cell. The oxygen extraction is performed using Aquanautics' proprietary oxygen absorbing carrier solution. This carrier solution is to be fed into the fuel cell directly where oxygen is chemically reduced in the cathode accompanied by oxidation of the hydrogen fuel to produce power.

Oxygen extraction from the seawater necessitates bringing the seawater and the carrier in close proximity with one another, so that net oxygen transfer can take place. An important characteristic that defines the choice of this unit is the need to keep the carrier and the seawater physically separate since mixing would dilute the aqueous carrier solution. As a consequence, membrane contactors were deemed necessary. Considerations of size and weight dictate the use of hollow fiber membranes which enable packaging of large interfacial areas in small volumes. The structure within which the hollow fiber membranes are implemented is called a gill because of its functional similarity to the breathing apparatus of fishes. In the system contemplated here, the carrier would be pumped through the lumen or the insides of the hollow fibers, while the seawater would flow on the outside of the fibers.

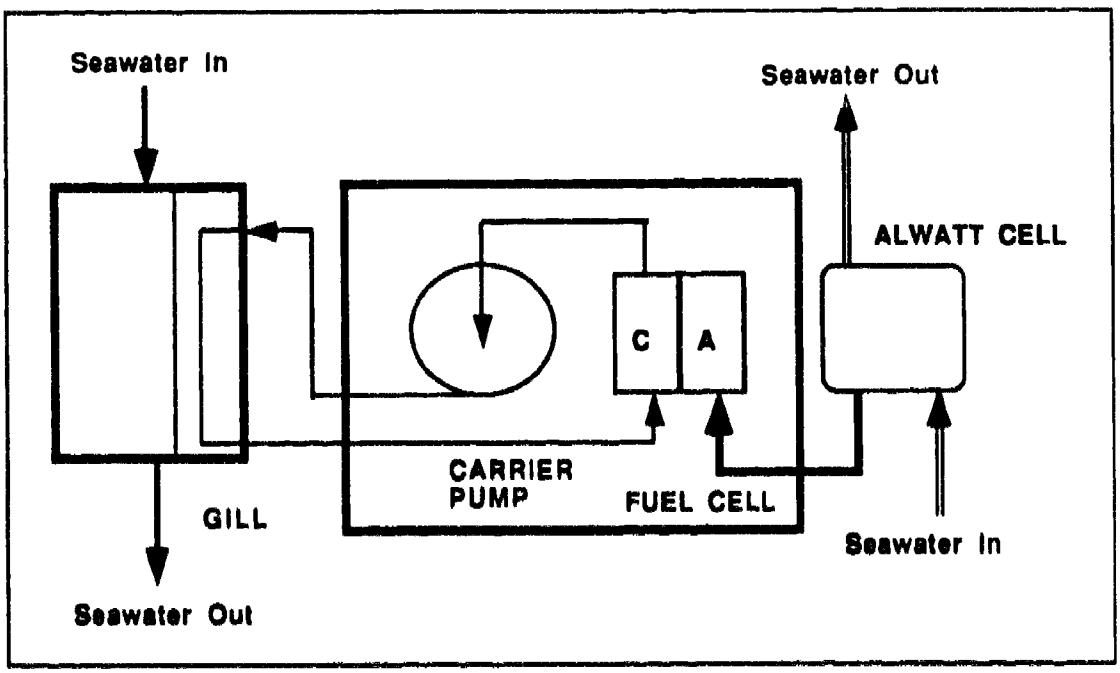

Figure 4.0.1 Schematic of an Undersea Power Source using Aquanautics' Oxygen Carrier

The system schematic for such a power system is depicted in Figure 4.0.1. The carrier solution is circulated by the carrier pump between the gill where it absorbs oxygen from the seawater and the fuel cell where the oxygen is used in the generation of power. The hydrogen for the fuel cell is evolved from an Aluminum-seawater battery which also

produces power. The power produced by the fuel cell is considered to be the net power output of the system. The power produced by the Aluminum-seawater battery, on the other hand, is used for the hotel loads of the system, which can be broadly divided into the following:

1) Carrier pump,
2) Seawater pump in the gill, and
3) Controls and Instrumentation.

Two considerations enter into the design of a power system using the Aquanautics oxygen extraction technology. The first consideration has to do with weight and volume. In order to be competitive with other systems, it is important that the Aquanautics system be smaller, both in weight and volume, when compared to existing technologies. The second consideration is that the power consumed by the various hotel loads described above be minimized. Because of the relative paucity of dissolved oxygen in seawater - typical concentrations range from 0.5 to 6 standard milliliters per liter of seawater - the seawater pumping power is expected to be the largest hotel load component. Therefore, system optimization has to proceed by examination of the gill volume and the seawater pumping power and investigation of the relationship between the two.

The purpose of this study is to describe a model which can be used to optimize the design of the gill component of the power system. This model quantifies the relationship between the seawater pumping power and the gill volume required to deliver a given oxygen flux rate.

4.1.0 Governing Equations

4.1.1 Description of Gill and Assumptions for the Model

It has been mentioned in the introduction to this study, that volume considerations dictate the use of hollow fiber contactors. Hollow fiber contactors are employed in a variety of arrays and present large interfacial areas packaged efficiently. Mass transfer across a hollow fiber membrane is dictated by the equation,

$$N = k A \Delta C$$

where, N is the flux of oxygen (mol/s),
k is the overall mass transfer coefficient (m/s)
A is the interfacial area or area of the gill membrane (m^2), and
ΔC is the difference in oxygen concentration between the seawater and the carrier (mol/m^3).

The mass transfer coefficient k is composed of three components. This is depicted in Figure 4.1.1. The three components are:

1) Carrier side mass transfer coefficient (k_c),
2) Membrane permeability (k_m), and
3) Seawater side mass transfer coefficient (k_s).

The overall mass transfer coefficient can be expressed as a function of its components by using the following relationship:

$$\frac{1}{k} = \frac{1}{k_c} + \frac{1}{k_m} + \frac{1}{k_s}$$

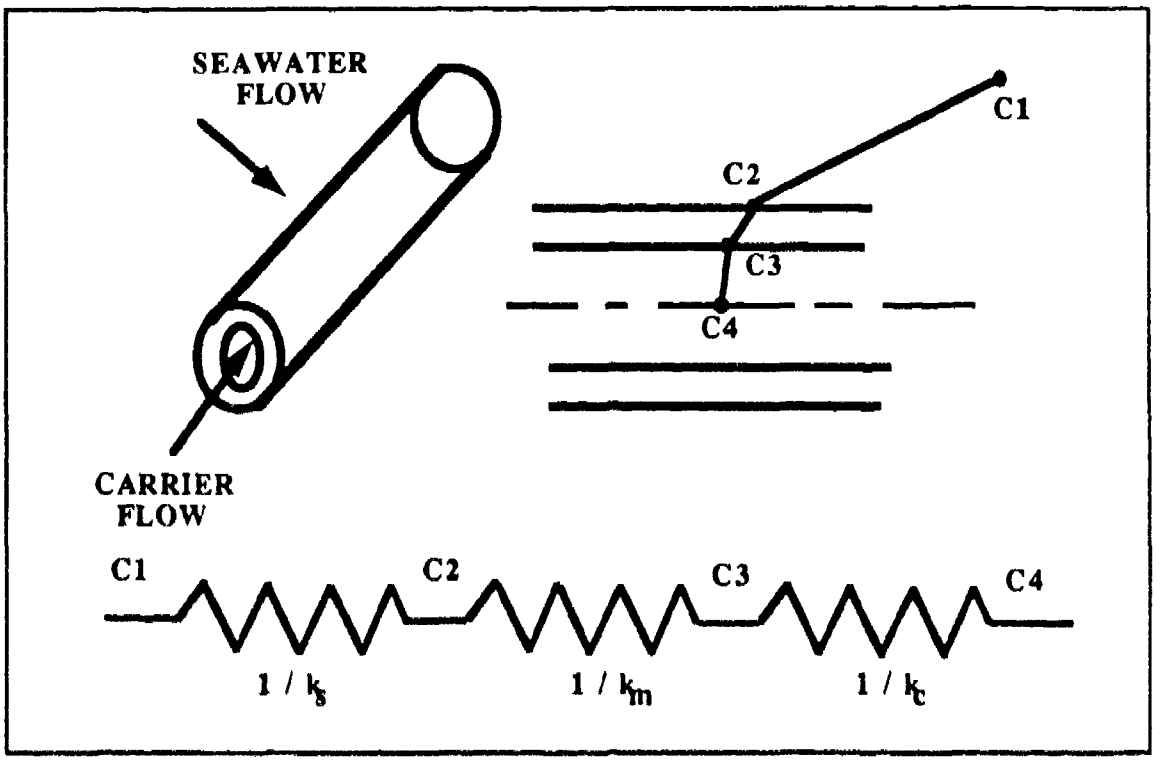

Figure 4.1.1 Schematic of Oxygen Diffusion through a Hollow Fiber Membrane

Of the three components that constitute the mass transfer coefficient k, the membrane permeability can be ignored because it is usually larger than the mass transport coefficient on the seawater side. This is because diffusion through liquids is much slower than it is through a thin membrane. On the carrier side, the concentration of dissolved oxygen is zero. This is because the oxygen that diffuses into the carrier from the seawater is immediately consumed in a chemical reaction where the carrier binds the oxygen. The system operates with an excess of deoxygenated carrier ensuring that the oxygen diffusing into the carrier is bound at all times, hence maintaining a concentration gradient at all points in the gill. The carrier side mass transport coefficient can therefore be ignored, since it is dictated by the reaction kinetics of carrier oxygenation, which is faster than the diffusion of oxygen through the seawater. Therefore, for purposes of engineering the artificial gill, it can be assumed that the overall mass transport coefficient is the same as the seawater side mass transport coefficient.

4.1.2 Theoretical Power-Volume Relationship

The design of a gill uses two types of tools. The first, derived from fluid mechanics, is the concept of a friction factor. The second, basic to mass transfer, is the idea of a mass transfer coefficient. The equations describing the two phenomena are introduced here and synthesized into one power-volume relationship.

A friction factor f is most commonly defined[3] in terms of a drag force F:

$$F = f\left(\frac{1}{2}\rho v^2\right)A \qquad (4.1.1)$$

where, f is a friction factor,
A is a characteristic area of the gill (m^2),
ρ is the density of the seawater (kg/m^3), and
v is the average velocity of the seawater flow through the gill (m/s).

What this characteristic area should be depends on the gill design. In the gills that are being considered for this application, sea water is pumped through narrow channels between hollow fibers. In this case, the dominant force is the drag in these channels, and the characteristic area is conventionally assumed to be that of outer surface of the gill membrane hollow fibers.

The mass transfer coefficient k, the second key tool, is defined in the equation for mass transfer,

$$N = k A \Delta C \qquad (4.1.2)$$

where, N is the oxygen flux rate (mol/s),
k is the mass transfer coefficient for the gill (m/s),
A is the surface area of the gill (m^2), and
ΔC is the concentration gradient across the gill (mol/m^3).

In this case, A is again the surface area of the gill membranes. The concentration differences ΔC, which is often called a "driving force," is in this case the actual oxygen concentration in the sea water minus that in equilibrium with the carrier solution. Since the oxygen diffusing into the carrier solution is bound immediately in a chemical reaction, the concentration of oxygen in the carrier can be assumed to be zero, and the value of the term ΔC becomes equal to the concentration of oxygen in the seawater.

These two ideas can be combined to determine the power required to pump seawater sufficient to allow for a given amount of mass transfer N. The seawater pumping power required to facilitate unit flux of oxygen can therefore be expressed by the ratio

$$\frac{P}{N} = \frac{vF}{N} = \frac{f\left(\frac{1}{2}\rho v^3\right)A}{k A \Delta C} \qquad (4.1.3)$$

where, P is the power required for seawater pumping through the gill (W).

The ratio of P to N should be minimized in an optimum gill design. To achieve this, Equation 4.1.3 is written in the form of a dimensionless equation,

[3] Baumeister, T., Avallone, E.A., and Baumeister, T., III, *Marks' Standard Handbook for Mechanical Engineers*, McGraw-Hill, New York (1978).

$$\left(\frac{P V^2}{\rho l^2 Q^3}\right) = \left(\frac{f v}{2 k}\right)\left(\frac{N}{Q \Delta C}\right) \qquad (4.1.4)$$

where, Q is the volumetric rate of flow of seawater through the gill (m^3/s),
V is the volume of the gill (m^3), and
l is the thickness of the gill in the direction of the seawater flow.

The volumetric flow Q is given by,

$$Q = V \frac{v}{l} \qquad (4.1.5)$$

For example, in the case of a shell and tube exchanger where seawater and carrier flow along parallel paths, the term l would refer to the length of the fibers. In the case of flow across a bed of fibers, where the seawater flows in a direction perpendicular to that of the carrier flow, the term l would indicate the thickness of the fiber bed.

This dimensionless equation contains three dimensionless groups. One of these [fv/2k], is the ratio of the friction factor to the Stanton number. This is also called the ratio of j-factors. For gases without form drag and in turbulent flow, this ratio is about one, an equality called the Reynolds analogy[4]. For liquids without form drag and in turbulent flow,

$$\frac{f v}{2 k} = \left(\frac{\upsilon}{D}\right)^{2/3} \qquad (4.1.6)$$

where, υ is the kinematic viscosity of the seawater (m^2/s), and
D is the diffusivity of oxygen through seawater (m^2/s).

This relation is called the Chilton-Coburn analogy. Similar relations are used in overwhelming detail for the design of compact heat exchangers. These results are largely restricted to turbulent flow. The non-dimensional group [fv/2k] has to be calculated for the artificial gills, where form drag and laminar flow are usually expected.

The second dimensionless group on the right hand side of Equation 4.1.4 is the oxygen extraction efficiency ($N/Q\Delta C$). This number is essentially the ratio of flux of oxygen to the rate at which it is presented to the gill. Clearly, when the driving force, which is given by the concentration difference ΔC, goes to zero, this number becomes large, and the power required will also become large.

The third dimensionless group $(PV^2/\rho l^2 Q^3)$ in Equation 4.1.4 represents the power to pump a certain amount of seawater, Q, through a gill of volume V and thickness l. This ratio is different than that used in conventional studies of mixing, where the impeller size and rotation are more directly considered. However, its physical significance is similar; it represents the ratio of power to flow within the gill. The importance of this and the other dimensionless groups will be clearer from the application of the general equation to the specific case of designing a gill. This process is discussed in the succeeding sections.

---

[4] Bennett, C.O., and Myers, J.E., *Momentum Heat and Mass Transfer*, McGraw-Hill, New York (1962).

4.1.3 Power-Volume Equation for Flow Across a Hollow Fiber Bed

Equation 4.1.4 from the previous subsection is of a general nature and the evaluation of the non-dimensional term [fv/2k] is dependent on the nature of the gill geometry and the mass transport characteristics associated with the geometry. Here the gill is assumed to consist of hollow fibers of outer diameter d_o that are laid against each other, with adjacent layers of hollow fibers running perpendicular to one another (see Figure 4.1.2). The overall geometry of the gill is such that the seawater flows through a square cross-section of area A_f and bed depth l. The cross-section of the gill is assumed to be square and of dimension a by a. The distance between adjacent fibers is given by ξd_o where ξ is a non-dimensional factor that defines the gap between the fibers. The volume of the gill is assumed to be V and the seawater flow rate Q. The oxygen extraction rate is assumed to be N.

It must be noted here that the velocity term v in Equation 4.1.3 as well as in the general form for the power (Equation 4.1.4) is the average interstitial seawater velocity through the gill. Because the entire gill cross section is not available for seawater flow due to the presence of the hollow fibers, the velocity cannot be calculated from the seawater flow rate Q and the frontal area of the gill A_f as in Equation 4.1.5. Instead, it has to be calculated from the actual area available for flow, namely A_a. The ratio of the frontal area to the available area is dependent on the fiber spacing factor as shown below,

$$\frac{A_f}{A_a} = \frac{\xi^2}{(\xi-1)^2}$$

where, ξ is the fiber spacing factor.

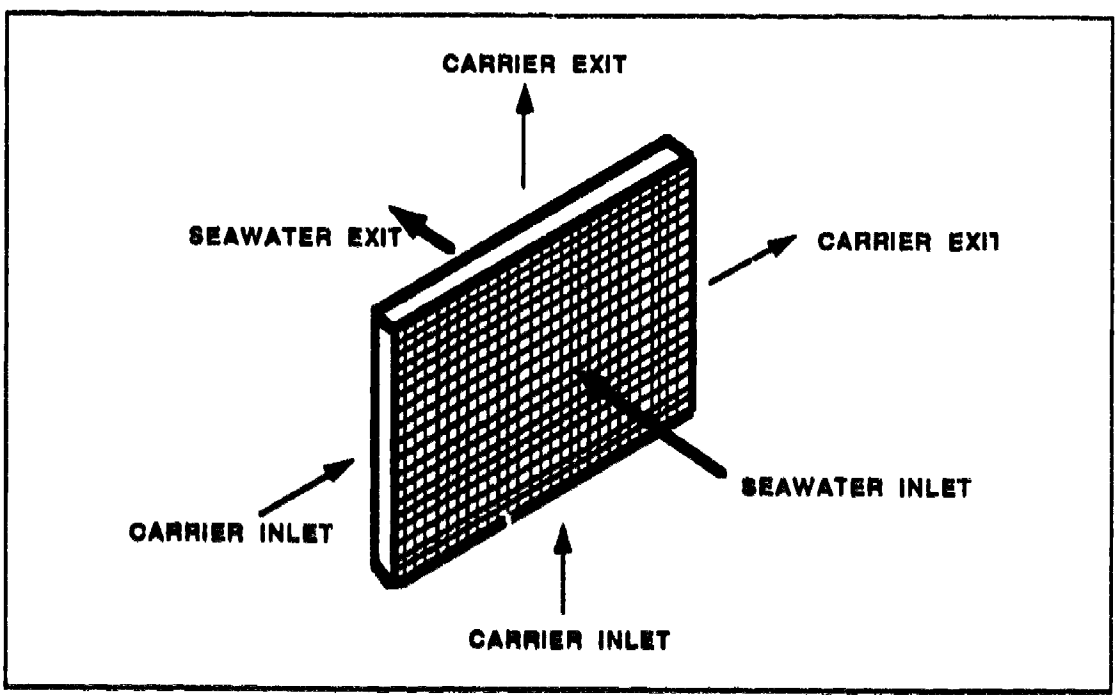

Figure 4.1.2 Preferred geometry for Gill

The velocity is therefore given by,

$$v = \frac{Q\, l\, \xi^2}{V\, (\xi-1)^2} \tag{4.1.7}$$

where, Q is the seawater flow rate (m^3/s),
V is the volume of the gill (m^3),
l is the thickness of the gill and the length of the seawater flow path (m), and
ξ is the fiber spacing factor.

When the expression for v given in Equation 4.1.5 is replaced with the expression given in Equation 4.1.7 the general expression for seawater pumping power becomes,

$$\frac{P\, V^2}{Q^3\, l^2\, \rho} = \left[\frac{\xi^4}{(\xi-1)^4}\right] \left[\frac{f\, v}{2\, k}\right] \left[\frac{N}{Q\, \Delta C}\right] \tag{4.1.8}$$

The friction factor f is a function of the Reynolds number and this relationship has been determined empirically for flow over banks of tubes. From the published data the friction factor for flow over a hollow fiber bed such as the one shown in Figure 4.1.2 can be defined as[5],

$$f = \frac{50}{Re} = \frac{50\, \upsilon}{v\, d_o} \tag{4.1.9}$$

where, υ is the kinematic viscosity of the seawater (m^2/s),
f is the friction factor, and
v is the velocity of the seawater through the gill (m/s).

For flow perpendicular to a hollow fiber, Yang and Cussler[6] have derived a correlation for the mass transfer coefficient k. The mass transfer coefficient can be determined from the Sherwood Number Sh which, for laminar flow (Re < 2000) of a liquid (Sc ≈ 1000) perpendicular to a hollow fiber array, is given by

$$Sh = 1.38\, Re^{0.34}\, Sc^{0.33}, \tag{4.1.10}$$

where, Re is the Reynolds Number ($v\, d_o/\upsilon$),
Sc is the Schmidt Number (υ/D), and
Sh is the Sherwood Number ($k\, d_o/D$).

For simplicity the exponent on the Reynolds Number is assumed to be 0.33 (introducing an error of approximately 1-5% in this case) also and the equation for k derived to be,

---

[5]Perry, R.H., and Green, D.W., *Chemical Engineers' Handbook*, McGraw-Hill, New York (1984).
[6]Yang, M.C., and Cussler, E.L.,"Designing Hollow-Fiber Contactors," *AIChE J.*, 32, 11 (1986)

$$k = 1.38 \frac{v^{(1/3)} D^{(2/3)}}{d_o^{(2/3)}} \qquad (4.1.11)$$

where, v is the seawater velocity as described in Equation 4.1.7 (m/s),
d_o is the outer diameter of the gill hollow fiber (m), and
D is the diffusivity of oxygen through seawater (m^2/s).

The expression for v from Equation 4.1.7 is used in Equation 4.1.11 to yield a new expression for the mass transfer coefficient shown in Equation 4.1.12.

$$k = 1.38 \frac{\xi^{(2/3)}}{(\xi-1)^{(2/3)}} \frac{Q^{(1/3)} l^{(1/3)} D^{(2/3)}}{V^{(1/3)} d_o^{(2/3)}} \qquad (4.1.12)$$

The outer diameter of the fiber can be expressed as a function of other parameters using Equation 4.1.2. The area of the gill A is expressed in terms of the number of fibers and the diameter of fibers using the expression

$$A = \pi d_o a n_t$$

where, a is the length of the fibers (m), and
n_t is the total number of fibers in the gill.

The total number of fibers in the gill can be calculated by multiplying the total number of fiber layers (in the direction of seawater flow) by the number of fibers per layer. Using a center to center distance of ξd_o for fibers in any given layer and assuming that adjacent layers lie against each other, the total number of fibers is found to be,

$$n_t = \frac{a\, l}{\xi\, d_o^2}$$

where, l is the thickness of the gill (m).

Substituting for n_t in the expression for the gill surface area yields the equation

$$A = \frac{\pi\, a^2\, l}{\xi\, d_o} = \frac{\pi\, V}{\xi\, d_o}$$

Using this expression for the gill surface area in Equation 4.1.2 yields an expression for the fiber outer diameter that is shown in Equation 4.1.13.

$$d_o = \frac{\pi\, k\, V\, \Delta C}{\xi\, N} \qquad (4.1.13)$$

where, k is the mass transfer coefficient on the seawater side (m/s),
ΔC is the oxygen concentration difference in the gill (mol/m^3), and
N is the oxygen flux rate (mol/s).

The volume of the gill, it must be recognized here, is the frontal area multiplied by the thickness of the gill and hence,

$$V = a^2 l$$

Using the expression for d_o to eliminate it from Equation 4.1.12 yields a new expression for the mass transfer coefficient shown in Equation 4.1.14.

$$k = 0.7675 \frac{\xi^{(4/5)}}{(\xi-1)^{(2/5)}} \frac{Q^{(1/5)} l^{(1/5)} D^{(2/5)} N^{(2/5)}}{V^{(3/5)} \Delta C^{(2/5)}} \qquad (4.1.14)$$

Equation 4.1.9 can be rewritten as,

$$\frac{f v}{2} = \frac{25 \upsilon}{d_o}$$

Eliminating d_o from the above equation (using Equation 4.1.13) and rearranging terms, yields an expression for the non-dimensional group [fv / 2k] as shown in Equation 4.1.15,

$$\frac{f v}{2 k} = 7.958 \frac{\upsilon \xi N}{k^2 V \Delta C} \qquad (4.1.15)$$

By substituting the expression for k from Equation 4.1.14 into the right hand side of Equation 4.1.15, a usable and final expression for [fv / 2k] is derived as shown in Equation 4.1.16.

$$\frac{f v}{2 k} = 13.5093 \frac{(\xi-1)^{0.8}}{\xi^{0.6}} \left(\frac{\upsilon}{D}\right) \left(\frac{V D}{Q l^2}\right)^{0.2} \left(\frac{N}{Q \Delta C}\right)^{0.2} \qquad (4.1.16)$$

This expression can now be substituted into the general equation for seawater pumping power (Equation 4.1.8) to yield Equation 4.1.17.

$$\frac{P V^2}{Q^3 l^2 \rho} = 13.5093 \frac{\xi^{3.4}}{(\xi-1)^{3.2}} \left(\frac{\upsilon}{D}\right) \left(\frac{V D}{Q l^2}\right)^{0.2} \left(\frac{N}{Q \Delta C}\right)^{1.2} \qquad (4.1.17)$$

4.1.4 Equation for Mass Transfer Across a Hollow Fiber Bed

The power-volume relationship expressed in Equation 4.1.17 does not constitute a well-posed problem because there are two unknowns. The intention of this modelling process is to determine the power needed to pump seawater through the gill as a function of the gill volume. In Equation 4.1.17, the values of the parameters D, ρ, and υ are given. These are properties of the seawater and are dependent primarily on the salinity and the temperature of the seawater. The value of the oxygen flux N depends on the desired capacity of the power generating unit. Further, the value of l, ξ, and d_o can be assumed. These represent the gill sizing parameters that define the hollow fiber arrangement and form the factors around which a gill can be optimized given the desired oxygen flux. Thus Equation 4.1.17 has three unknown quantities namely ΔC, Q, and P. The concentration

difference and the seawater flow rate are, however, related through the oxygen flux equation (Equation 4.1.2) and therefore the term ΔC can be expressed in terms of the seawater flow rate Q. This leaves the two unknowns, namely Q and P.

In order to obtain the power required for seawater pumping, the value for the seawater flow rate sufficient to provide the desired flux has to be calculated independently. Fortunately, this is possible by resolving Equation 4.1.2 to yield a second equation relating Q to V. The derivation of such an equation would yield a well posed problem with two unknowns and two equations.

The concentration difference term in the last non-dimensional group in Equation 4.1.17 is usually of a log-mean difference form given by,

$$\Delta C = \frac{(C_{si} - C_{co}) - (C_{so} - C_{ci})}{\ln\left(\frac{C_{si} - C_{co}}{C_{so} - C_{ci}}\right)} \qquad (4.1.18)$$

where, C_{si} is the oxygen concentration in the seawater at the gill inlet,
C_{so} is the oxygen concentration in the seawater at the gill exit,
C_{ci} is the oxygen concentration in the carrier at the gill inlet, and
C_{co} is the oxygen concentration in the carrier at the gill exit.

All the concentration terms in Equation 4.1.18 are expressed in terms of mols/m^3. The oxygen concentration in the carrier can be assumed to be zero at all locations in the gill, since we are assuming that an excess of carrier is being supplied to the gill. This means that the oxygen that enters the carrier in solution through the membrane is immediately bound chemically by the deoxygenated carrier molecules that exist in abundance. This assumption permits ignoring the carrier side mass transport coefficient when calculating the seawater pumping power. Therefore the terms C_{ci} and C_{co} are eliminated from Equation 4.1.18 to give a new expression for the concentration gradient,

$$\Delta C = \frac{C_{si} - C_{so}}{\ln\left(\frac{C_{si}}{C_{so}}\right)} \qquad (4.1.19)$$

The terms C_{si} and C_{so} can also be related to the oxygen flux and the seawater flow rate by the equation,

$$N = Q(C_{si} - C_{so}),$$

which when rearranged yields,

$$C_{so} = C_{si} - \frac{N}{Q}. \qquad (4.1.20)$$

When this expression for C_{so} is substituted into Equation 4.1.19 and the term ΔC in Equation 4.1.17 replaced with the expression from Equation 4.1.19, the new power equation becomes,

$$\frac{P\,V2}{Q^3\,l^2\,\rho} = 13.5093\,\frac{\xi^{3.4}}{(\xi-1)^{3.2}}\left(\frac{\upsilon}{D}\right)\left(\frac{V\,D}{Q\,l^2}\right)^{0.2}\left(\ln\frac{C_{si}}{C_{si}-\frac{N}{Q}}\right)^{1.2} \qquad (4.1.21)$$

A new version of the mass transport equation is now developed to relate the flux N with the seawater flow rate Q for the given gill design and volume. This is done by replacing the terms k, ΔC, and A in Equation 4.1.2. To do this a new expression for the surface area A is determined from the relations for A and n_t in the preceding section.

$$A = \frac{\pi\,V}{\xi\,d_o}$$

An expression for the term ΔC is determined by substituting the value for C_{so} from Equation 4.1.20 in Equation 4.1.19. When the new expressions for A and ΔC are introduced into Equation 4.1.2 along with the expression for k from Equation 4.1.12 a new expression for the flux N results as shown in Equation 4.1.22.

$$N = 1.38\,\frac{1}{\xi^{(1/3)}\,(\xi-1)^{(2/3)}}\,\frac{\pi\,D^{(2/3)}\,V^{(2/3)}\,l^{(1/3)}}{Q^{(2/3)}\,d_o^{(5/3)}}\,\frac{N}{\ln\left\{\frac{C_{si}}{C_{si}-\frac{N}{Q}}\right\}} \qquad (4.1.22)$$

By eliminating the quantity N from both sides of Equation 4.1.22 an expression for the last non-dimensional group of Equation 4.1.21 can be determined as shown in Equation 4.1.23.

$$\ln\left\{\frac{C_{si}}{C_{si}-\frac{N}{Q}}\right\} = 4.3354\,\frac{1}{\xi^{(1/3)}\,(\xi-1)^{(2/3)}}\,\frac{D^{(2/3)}\,V^{(2/3)}\,l^{(1/3)}}{Q^{(2/3)}\,d_o^{(5/3)}} \qquad (4.1.23)$$

The value for Q is independently determined from Equation 4.1.23, given the geometry of the gill (represented by V, d_o, l and ξ), in situ properties of the seawater (represented by C_{si} and D) and the flux desired, N. This value for the seawater flow rate Q is then introduced into Equation 4.1.21 and the value for P calculated. A parametric analysis can be performed by changing the input values of the gill sizing parameters, V, d_o, l, and ξ to identify the optimum gill configuration. Equations 4 '.21 and 4.1.23 therefore form a well posed problem where the two unknowns Q and P are evaluated as functions of V.

4.2.0 Application of the Gill Power-Volume Model

The gill power-volume model was applied and a parametric analysis performed for a one standard liter per minute gill. The study was intended to identify the effect of the parameters that define a gill design on the power to pump the seawater through the gill. The various values for which the model was applied are shown in Table 4.2.1, and the baseline values for the various parameters have been indicated. For example, the variation of P as a function of V was studied for four different values of ξ keeping the other

parameters constant at their baseline values. This process was repeated for each individual parameter, l, d_o, and C_{sl}.

TABLE 4.2.1

l (cm)	d_o (microns)	ξ	C_{sl} (ml/l)	Comments
5.0	300	2.0	3.00	Baseline
2.5	400	3.0	1.50	
7.5	500	4.0	2.25	
10.0	600	5.0	4.50	

The effects of the various parameters on the power for seawater pumping are presented in sections below. Along with the power for seawater pumping, two other parameters namely seawater flow rate and the pressure drop through the gill were also evaluated. The seawater flow rate required for a given oxygen flux was computed from Equation 4.1.23 for various values of gill volume, and the value for the seawater pumping power calculated by substituting this value for Q into Equation 4.1.21. The value for the pressure drop through the gill was computed from the pumping power and the flow rate using the equation,

$$\Delta p = \frac{P}{Q} \qquad (4.2.1)$$

where, Δp is the pressure drop through the gill (N/m^2), and
P and Q are as defined before.

4.2.1 Effect of Gill Fiber Outer Diameter

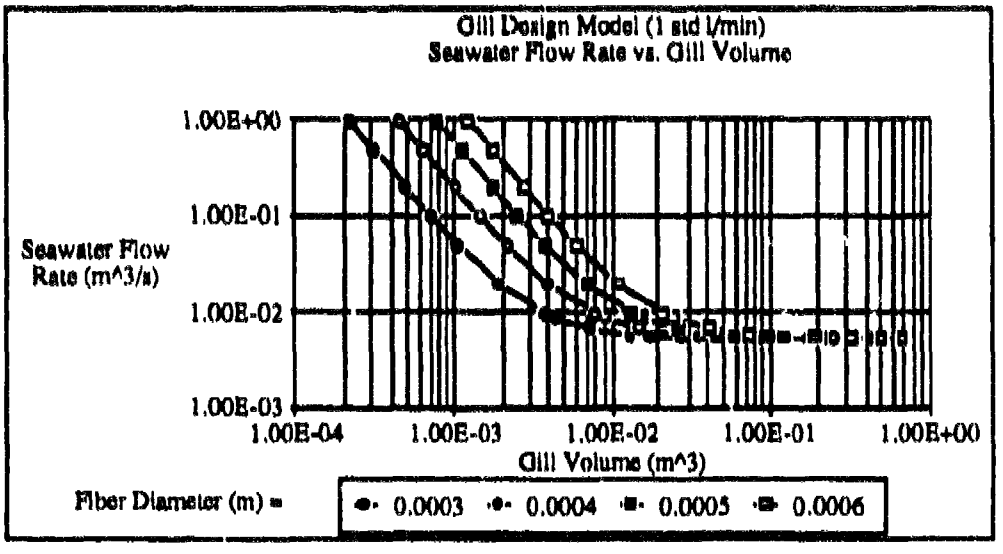

Figure 4.2.1 Seawater Flow Rate for Various Gill Fiber Outer Diameters

Figures 4.2.1, 4.2.2, and 4.2.3 depict the variation of the seawater flow rate, seawater pumping power, and seawater pressure drop respectively as a function of the gill volume. The graphs show this variation for the four different values of the fiber outer diameter listed in Table 4.2.1. The calculations were done with the other parameters (ξ, l, and C_{si}) at their respective baseline values shown in Table 4.2.1. The fiber outer diameters in the legends of these graphs are in units of meters.

It is clear from Figure 4.2.1 that as the volume of the gill is increased for a particular value of the fiber outer diameter, the flow rate required for an oxygen flux of 1 standard liter per minute decreases. This is because a larger gill packs a greater surface area of membrane and therefore requires smaller seawater velocities for the same flux. It is also apparent that as the fiber outer diameter increases, the flow rate corresponding to a particular gill volume increases. This happens because for the same gill volume and spacing factor ξ the larger fibers mean a smaller membrane surface area, and hence a greater required seawater velocity. It is interesting to note from Figure 4.2.1, however, that the seawater flow rate reaches an asymptotic minimum for gill volumes greater than approximately 0.1 m^3. This is reflective of the fact that for large gills, the large surface area and high residence times combine to ensure close to 100% oxygen extraction. The asymptotic minimum therefore reflects the minimum amount of seawater flow rate required given its initial oxygen concentration and the oxygen flux.

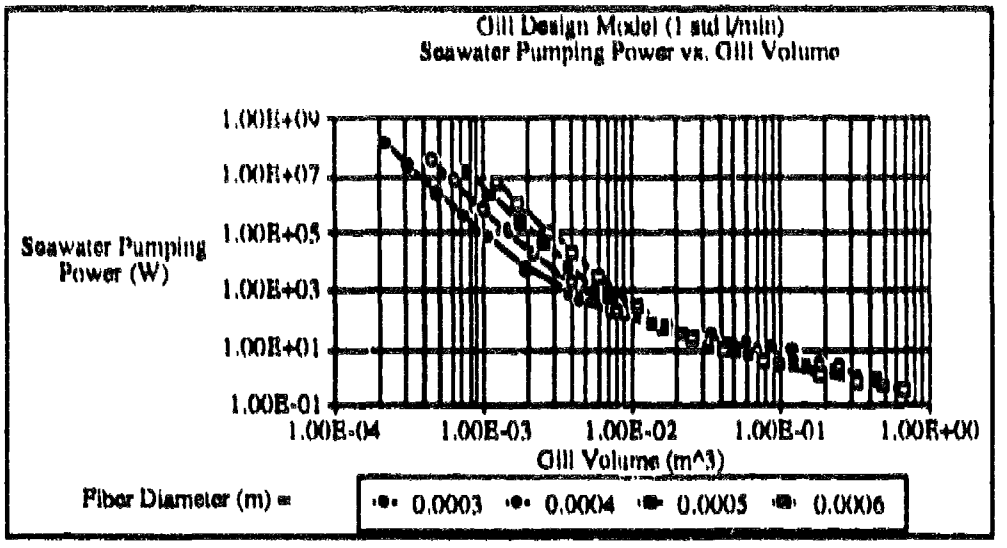

Figure 4.2.2 Seawater Pumping Power for Various Gill Fiber Outer Diameters

Figure 4.2.2 depicts the variation of the seawater pumping power as a function of the gill volume for various fiber sizes. As expected, the pumping power decreases as the volume increases. At the lower end of the gill volume spectrum, the power to pump seawater through the gill goes up as the fiber diameter increases. This is because the smaller area presented by the larger fibers dictates that larger quantities of seawater be pumped through the gill. At higher values of gill volume, however, the converse is true. Larger fibers in this case lead to smaller values of pumping power. This is because of the fact that the seawater flow rate has reached its asymptotic minimum and 100% extraction is being effected. Therefore, the seawater pumping power becomes solely dependent on the space

between the gill fibers and this space is larger for larger fibers owing to the fact that the value for ξ is constant.

Figure 4.2.3 is a graph showing variation of the pressure drop through the gill as a function of gill volume for various gill fiber sizes.

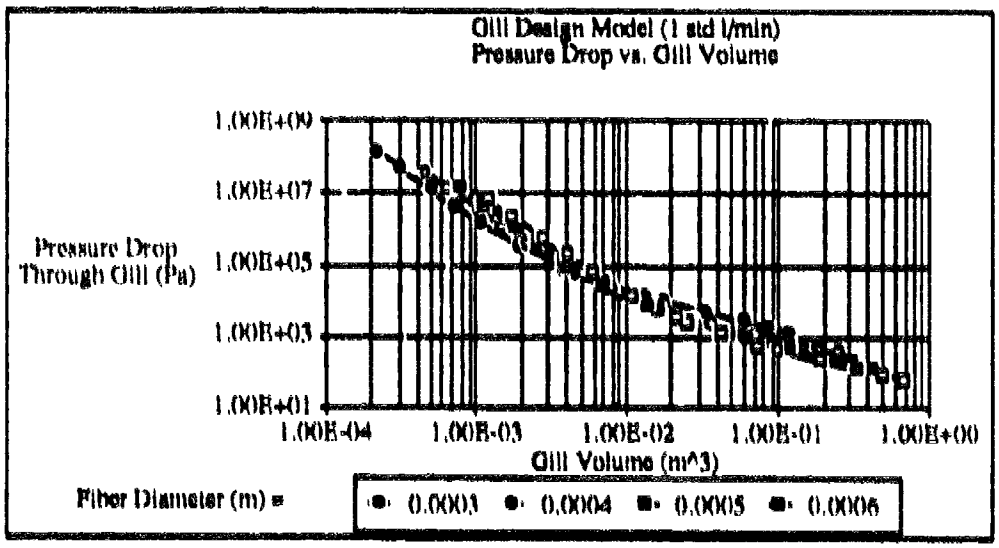

Figure 4.2.3 Pressure Drop for Various Gill Fiber Outer Diameters

4.2.2 Effect of Gill Fiber Spacing

Figures 4.2.4, 4.2.5, and 4.2.6 depict the variation of the seawater flow rate, seawater pumping power, and the pressure drop through the gill respectively as a function of the gill volume for various values of the gill fiber spacing factor ξ. The values of the other variables, namely d_o, l, and C_{sl} were held constant at their respective baseline values.

Figure 4.2.4 depicts the variation of the seawater flow rate as a function of the gill volume for four different values of the gill spacing factor. The flow rate is shown to increase for larger spacing and this is because the larger spacing implies smaller membrane surface areas within the same gill volume. Therefore larger seawater velocities have to be attained in order to facilitate the desired oxygen flux. As in the previous case (see Figure 4.2.1), the seawater flow rates attain an asymptotic minimum when the gill volume exceeds approximately 0.1 cubic meters. Once again, for large volumes, the flow rate is so low that virtually all the oxygen in the seawater is extracted and therefore the flow rate is limited primarily by the initial oxygen concentration and the desired oxygen flux.

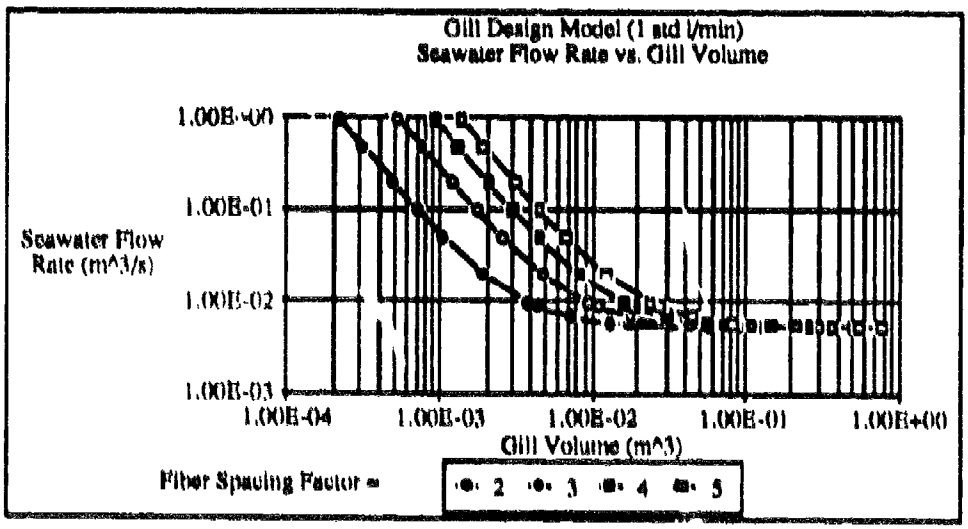

Figure 4.2.4 Seawater Flow Rate for Various Gill Fiber Spacing Factors

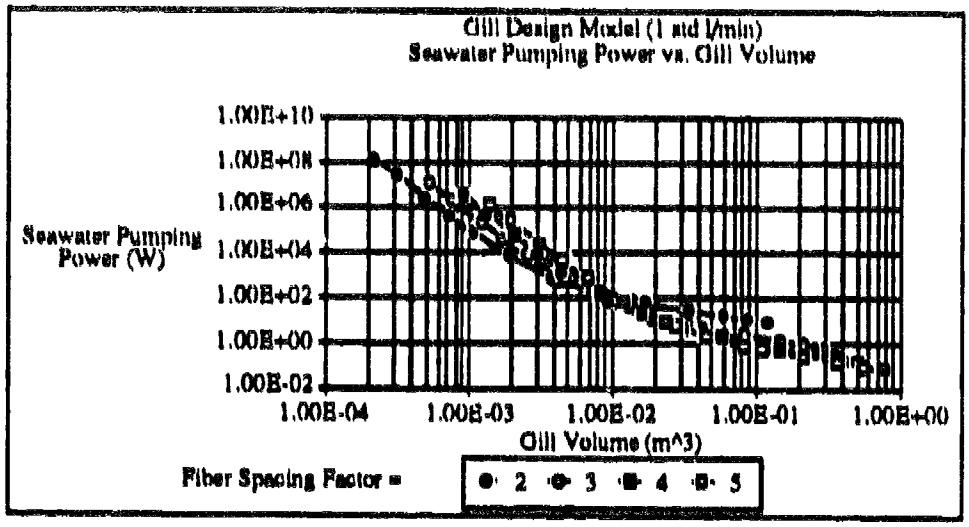

Figure 4.2.5 Seawater Pumping Power for Various Gill Fiber Spacing Factors

Figure 4.2.5 represents the pumping power variation as a function of the gill volume for the various gill spacing factor values. This graph is similar to that in Figure 4.2.2, in that the pumping power is higher for larger values of gill spacing when the gill volume is small. This is because of the smaller membrane areas implied in larger gill spacing factors, which in turn, necessitates larger seawater flow velocities and higher flow rates. At higher gill volumes, the converse is true, i.e., the pumping power is smaller for larger fiber spacing. This is because the seawater is being exhausted of all oxygen at this point and therefore, the required flow rate is constant regardless of the spacing factor. The larger spaces between the gills imply reduced drag and correspondingly smaller pumping power values.

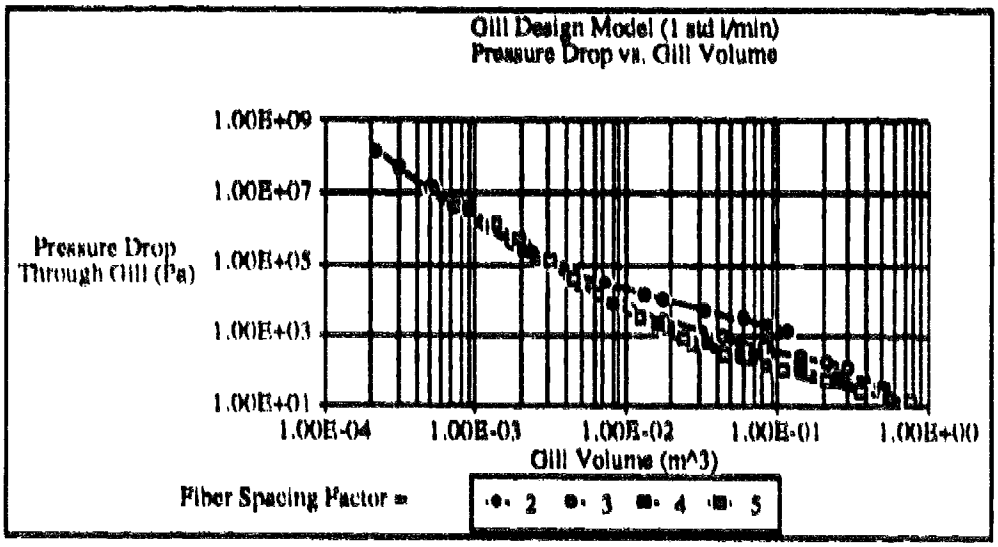

Figure 4.2.6 Pressure Drop for Various Gill Fiber Spacing Factors

Figure 4.2.6 depicts the variation of the gill pressure drop for different values of the gill spacing factor.

4.2.3 Effect of Gill Fiber Bed Thickness

The effect of the gill fiber bed thickness l is examined in Figures 4.2.7, 4.2.8, and 4.2.9 which represent the variation of the seawater flow rate, seawater pumping power and the pressure drop respectively as a function of the gill volume. These calculations have been done with the other variables, namely d_O, ξ, and C_{gl} at their baseline values as shown in Table 4.2.1.

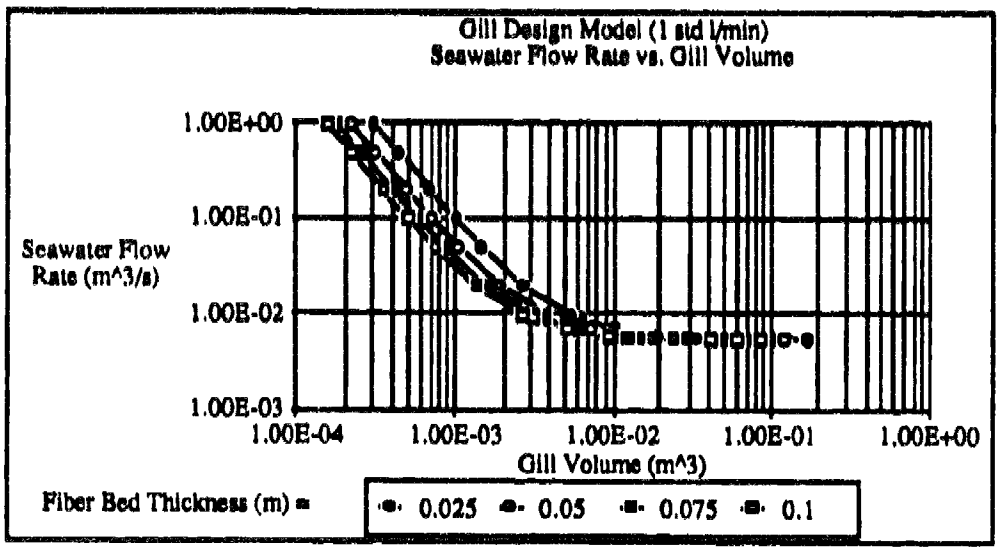

Figure 4.2.7 Seawater Flow Rate for Various Gill Thickness Values

Figure 4.2.7 shows the variation of the seawater flow rate as a function of gill volume for various values of the gill thickness ranging from 2.5 cm to 10 cm. The gill was again sized for an oxygen flux of one standard liter per minute. Figure 4.2.7 shows that the seawater flow rate required for the above flux decreases with increasing gill thickness. This can be attributed to the fact that by increasing the gill thickness, a greater proportion of the oxygen present in the seawater is extracted. Therefore a smaller rate of seawater flow is required for gills with thicker fiber beds. As in the previous cases, the seawater flow rate reaches an asymptotic value beyond a certain value of gill volume. This asymptotic value again corresponds to the situation in which close to 100% of the oxygen is extracted from the seawater as described in the preceding sections.

The model for the oxygen transport across the membrane assumes a logarithmic profile for the concentration difference ΔC along the thickness of the fiber bed. This means that the fibers in the front portion of the gill perform most of the work as far as oxygen extraction is concerned. Because of this, adding to the thickness of a gill does not contribute very much to the extent of oxygen extraction, especially at higher gill volumes.

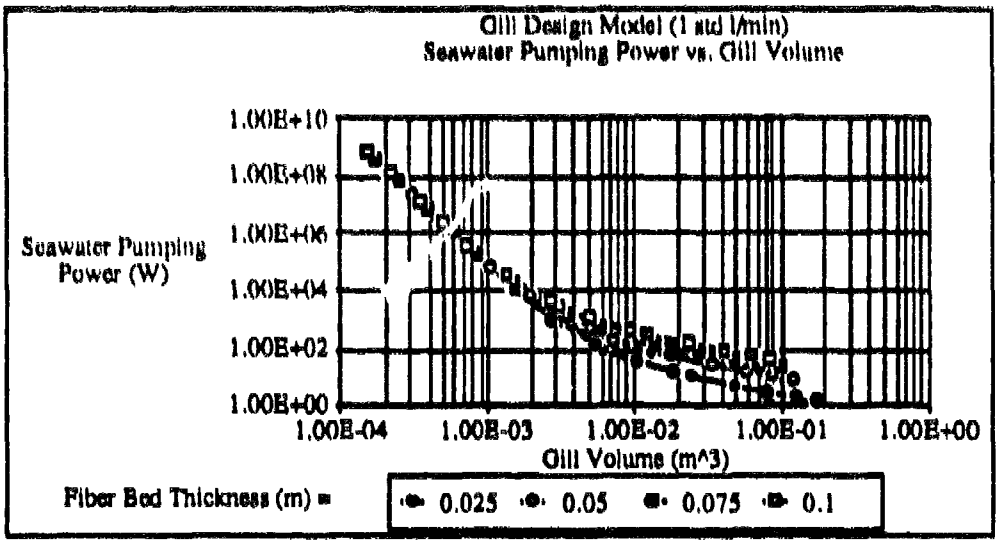

Figure 4.2.8 Seawater Pumping Power for Various Gill Thickness Values

Figure 4.2.8 depicts the variation of the seawater pumping power as a function of the gill volume. As expected, the pumping power is lowest for gills with the smallest fiber bed thicknesses. The pumping power at the lower extreme of the volume scale is, however, independent of the thickness. This is because the positive contribution - to the seawater pumping power - of increased frontal area and shorter seawater path length in gills with thinner fiber beds, is cancelled by the larger seawater flow rate required. However, the larger frontal area and smaller path length associated with thinner gills do produce power savings in gills with high volumes. This is because the virtual depletion of the seawater in large gills dictates that the flow rate be independent of the gill thickness. Hence, it can be seen from Figure 4.2.8, that for large gills, a thinner fiber bed would offer advantages with regard to savings in seawater pumping power.

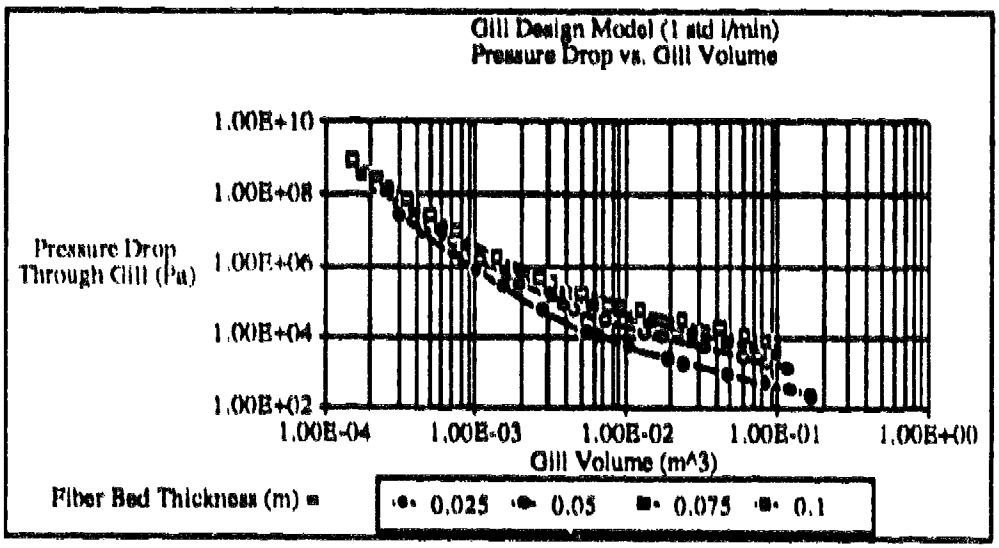

Figure 4.2.9 Pressure Drop for Various Gill Thickness Values

4.2.4 Effect of Initial Oxygen Content of Seawater

The effect of the initial oxygen concentration in seawater is examined in Figures 4.2.10 through 4.2.12. Concentrations are expressed in standard ml of O_2 per ml of seawater. The values of d_o, ξ, and l were held constant at their baseline values for this set of calculations.

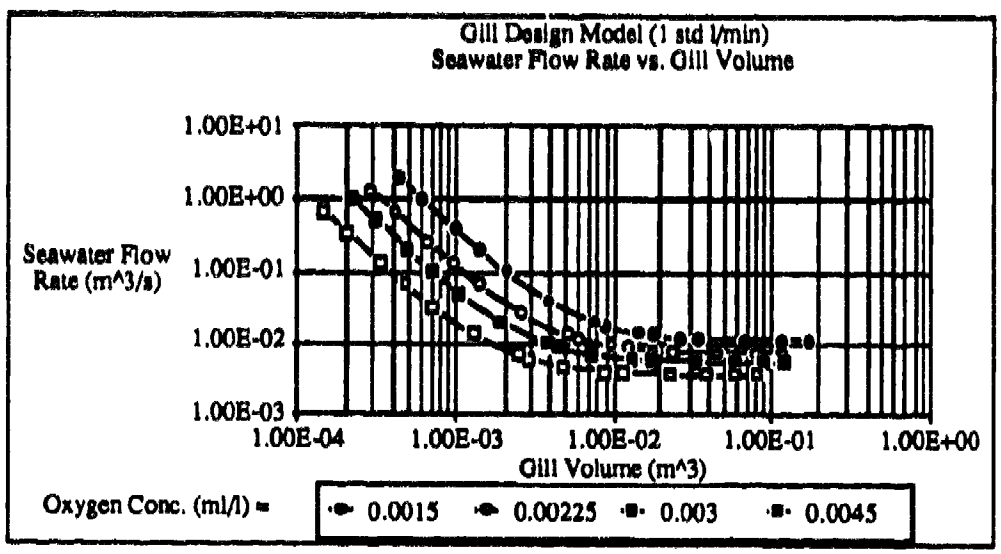

Figure 4.2.10 Seawater Flow Rate for Various Seawater Oxygen Concentrations

Figure 4.2.10 shows the variation of the seawater flow rate required for one standard liter per minute oxygen flux as a function of the gill volume. It is apparent that as the initial oxygen concentration decreases, it is necessary to pump larger quantities of seawater through the gill. The asymptotic minimum for the seawater flow rate is different for each value of the initial seawater oxygen content. This is to be expected from the fact that the

asymptotic minimum represents 100% extraction of oxygen and therefore the flow rate necessary to produce the desired flux would depend only on the initial oxygen content of the seawater.

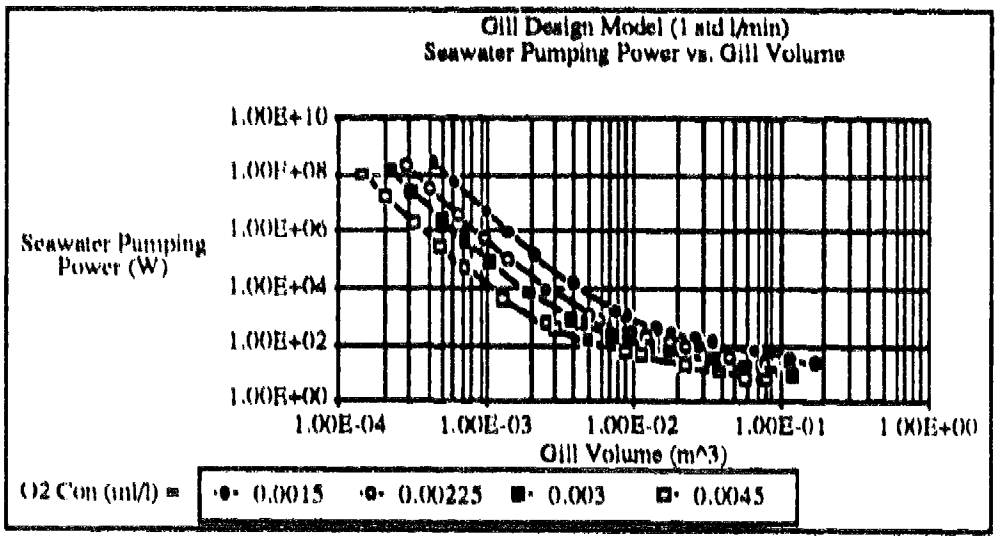

Figure 4.2.11 Seawater Pumping Power for Various Seawater Oxygen Concentrations

The variation of the seawater pumping power as a function of the gill volume for various values of C_{sl} is investigated in Figure 4.2.11. It is apparent that the pumping power required for conditions of lower oxygen concentration is higher than that for oxygen-rich environments.

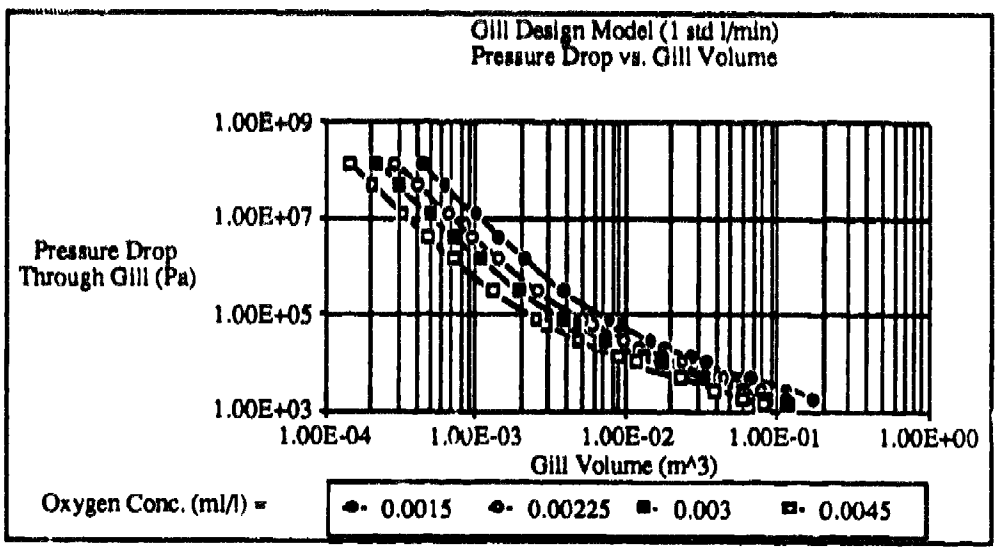

Figure 4.2.12 Pressure Drop for Various Seawater Oxygen Concentrations

Figure 4.2.12 shows the pressure drop variation as a function of the gill volume for various values of the initial oxygen concentration in seawater.

4.3.0 Gill Optimization

The DARPA project calls for the utilization of a gill to extract oxygen from the seawater for use in a stationary power source. The best design of such a power source would imply the choice of a gill that uses the least amount of power for seawater pumping. Ideally a power system would not require any seawater pumping at all, but would rely on the existing seawater currents for oxygen extraction. However, given the paucity of information regarding the magnitude of such seawater currents and their transient nature it is recommended that a power system designed around a gill have a seawater pump. Since it is desired that this gill operate at the lower end of the power consumption spectrum, it is likely to be of relatively large volume. Figures 4.2.2, 4.2.5 and 4.2.8 investigated the power consumption of a gill for various values of d_o, ξ, and l. It was found from the first two graphs that larger fibers and larger interstitial spaces do not automatically mean higher pumping powers. Intuitively, it is apparent that the larger gill fiber and spacing factor contribute to reduced surface area available for mass transport in a given volume, and therefore, higher seawater pumping power. This higher seawater pumping power would be associated with increased seawater flow rates and in turn higher seawater velocities to overcome the effect of the reduced surface areas.

However, the model actually predicts lower pumping powers for larger values of d_o and ξ when the volume of the gill is large. This anomaly was explained as being due to the complete extraction of oxygen from seawater. The exhaustion of the seawater oxygen content is due to the comparatively large volume of the gill and consequently its large surface area. However, if this analysis is extended for ever increasing values of d_o and ξ, it becomes apparent that there should be a limit to the decrease in seawater pumping power. In other words, the power would decrease as the values of d_o and ξ are increased, up to a certain point, beyond which the surface area reduction would start to predominate and the conditions of 100% extraction would no longer exist.

This means that in the range of gill volumes considered ideal for this application, it is possible to optimize the values of d_o and ξ so as to obtain a design requiring minimum amount of power. The most likely process of design would commence from deciding upon an allocation of power for seawater pumping. Accordingly the gill design optimization process is illustrated here by using the following assumptions:

Gill Pumping Power	=	P	=	10 W
Oxygen Flux Desired	=	N	=	1 standard l/min
Initial Oxygen Concentration	=	C_{si}	=	3 standard ml/ml of seawater
Seawater Viscosity	=	υ	=	1.7621 E-06 m^2/s
Diffusivity of oxygen in seawater	=	D	=	2.1 E-09 m^2/s
Density of seawater	=	ρ	=	1025.8 kg/m^3

With these assumptions in mind the gill design was optimized using Equations 4.1.21 and 4.1.23. The process commenced by solving both equations simultaneously using the Newton-Raphson method to find values for V and Q given the value for P.

4.3.1 Optimization of Gill Volume With Respect to d_o

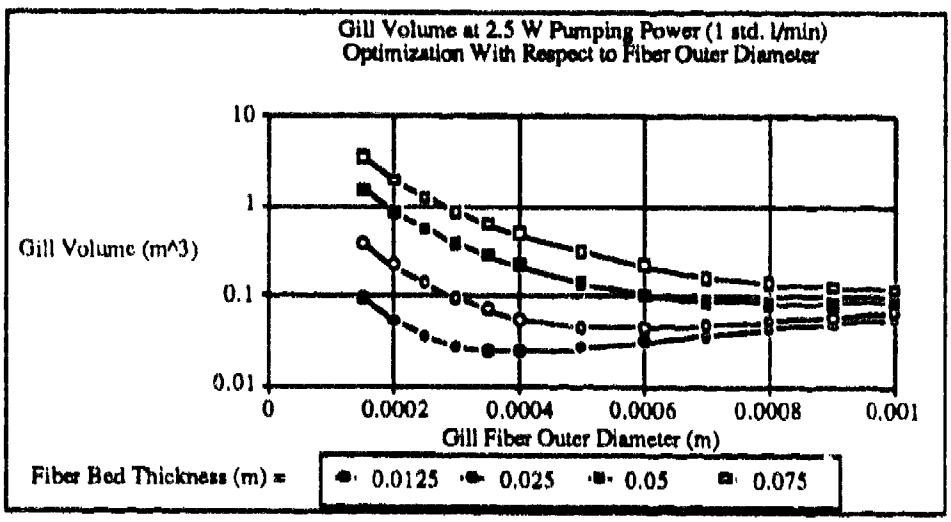

Figure 4.3.1 Gill Volume as a function of d_o for fixed Pumping Power

Figure 4.3.1 depicts the volume of a gill consuming 10 W to produce 1 l/min of oxygen given the conditions listed above. The volume is plotted as a function of the gill fiber outer diameter for various values of the fiber bed thickness l (units in the legends are meters). The gill fiber spacing factor ξ was kept constant at a value of 2 for this analysis. It can be seen from Figure 4.3.1 that for each value of the variable l, the gill volume has a minimum value. The fiber diameter corresponding to the minimum gill volume changes with the bed thickness. This graph should therefore constitute a design tool for the selection of a fiber size given the desired oxygen flux and the pumping power allocated for moving the seawater.

4.3.2 Optimization of Gill Volume With Respect to ξ

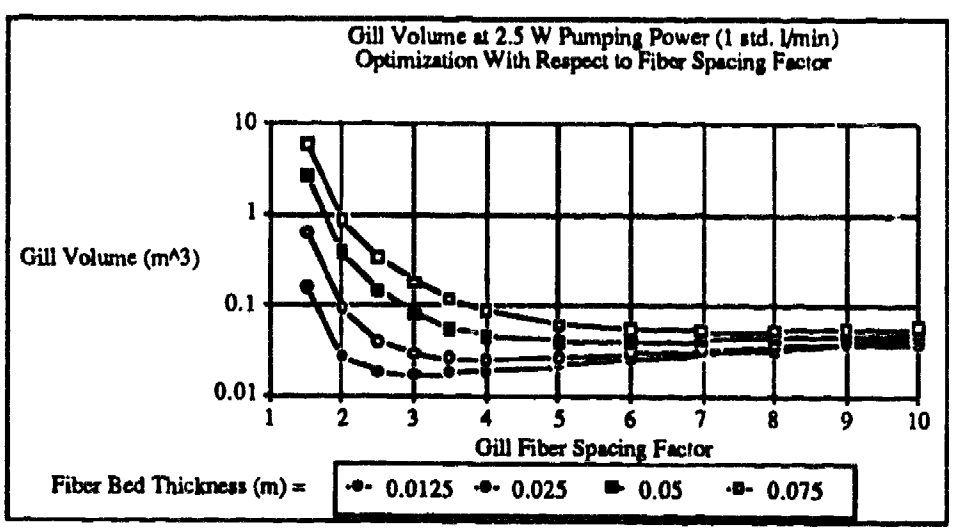

Figure 4.3.2 Gill Volume as function of ξ for fixed Pumping Power

Figure 4.3.2 depicts the variation of the gill volume V as a function of the gill fiber spacing factor ξ for various values of l (units in the legend are once again in meters). As in the case with d_o, the gill volume is shown to have a minimum value. The value for ξ at which this minimum gill volume is realized also depends on the value for the variable l. Together with the graph shown in Figure 3.1, this graph should constitute a complete gill design tool with the ability to specify the four important gill design parameters, namely V, l, d_o, and ξ.

4.4.0 Conclusions

The design of a gill for the power system is crucial in as far as maintaining a size and cost advantage with respect to other technologies is concerned. The proper design of a gill specific to the conditions at the site of installation should help keep the system volume down and minimize the seawater pumping power required. These goals form the basis of establishing the feasibility of the system as well as comparing its performance characteristics with respect to other technologies.

In designing a gill, a number of phenomena have to be considered and modelled. It is also important that the model for the gill be easily implemented and be self-sufficient in terms of minimizing the number of assumptions. The model proposed in this study does just that. The twin phenomena of drag and oxygen diffusion are considered and implemented into a set of two simultaneous equations. These equations form a well-posed problem that can be solved without the need to make extraneous assumptions. Moreover the equations lend themselves to parametric analysis thus helping analyze the importance of the various gill sizing parameters and also assisting in the identification of suitable values for these parameters.

The sensitivity analysis and the gill optimization exercise undertaken as part of this study have yielded general purpose spreadsheet models that can be employed as part of larger system sizing models. This study has also demonstrated that there exists a region defined by values of the gill fiber diameter and the fiber spacing factor that allows for minimum volume at a given pumping power and flux rate. This region is specific to the oxygen content of the seawater and therefore the model allows flexibility in designing gills specifically for the in situ values of oxygen concentration at the site of application.

Further work on the gill design is intended to experimentally verify the results of the model developed here. Experimental verification shall be performed in the laboratory with the help of gill cartridges that are being constructed under the DARPA project. Eight cartridges in all encompassing two variables are being built. Of the eight cartridges, four shall consist of microporous hollow fiber membranes, while four shall be constructed from solid hollow fiber membranes. The solid membrane represents the coating of a conventional microporous membrane with a proprietary oxygen permeable polymer to help prevent pore collapse and liquid-liquid contact at high pressures. Within the four cartridges of each type, two values of the fiber spacing factor ξ shall be used. These values will be 1.5 and 2.5. These variations shall help verify the effect of the fiber spacing factor as predicted by the model.

In the experiments, the carrier shall be pumped through the insides of the fibers and the seawater through the fiber bed on the outside. By measuring the flow rate of the seawater, the pressure drop in the seawater flow across the fiber bed, and the decrease in oxygen content of the seawater, the model shall be verified and calibrated.

5.0 DIRECT FEED FUEL CELL INTEGRATION WITH SEAWATER LOADER

An integration of the solid membrane gill module with the direct feed fuel cell was carried out in order to ascertain that the two subsystems are compatible and that their individual performance is not compromised by their interaction.

The intention of the integration was to replicate the conditions used in the previous gill and fuel cell experiments. However several experimental conditions were not duplicated. First, due to an error in reading a rotometer (stainless steel ball instead of glass) the carrier flow rate through the gill was about three times higher than had previously been used. Second, fuel cell experiments had not previously been run at the temperatures used in the gill experiments. Third, fuel cell experiments had not previously been run using carrier solutions without supporting electrolyte as used in the gill experiments. These differences are reflected in the results of the integration study.

5.1 Fuel Cell Performance

The cell voltage at 4 mA/cm^2 in the integration experiment was 0.19 volts as compared to 0.25 in the reference experiment. The difference can be accounted for in part by the differences in temperature and conductivity. The difference in temperature accounts for approximately 15 mV ($\Delta V = 0.25 (1 - (277°K/ 295°K))$. The difference in conductivity accounts for about 13 mV in cell iR. The difference is estimated by correcting the measured conductivities to 5°C and 42 mmho/cm at 16°C is about 33 mmho/cm at 5°C). Then multiplying the measured iR by the inverse ratio of the conductivities ($\Delta V = 0.02 (1 - (33/90)$. The difference in conductivity will however result in a larger difference in cell voltage than the iR difference alone since the reaction distribution in the felt electrode will be different. This additional effect is difficult to estimate but could very well account for the additional 32 mV difference in cell performance. Subsequent fuel cell experiments will examine the effect of conductivity on cell performance.

5.2 Gill Performance

The gill performance in terms of maximum oxygen transport, milliliters per minute per square meter, was found to be 3.6 versus 2.6 in a previous experiment with the same seawater flow rate (1.34 liters per minute per square meter). However the carrier flow rate in the previous experiment was 0.134 lpm/m^2 versus 0.323 lpm/m^2 in the integration. The difference in oxygen flux can perhaps be explained by the difference in flow rate.

The maximum oxygen flux was measured while the carrier was becoming oxygenated before steady state system operation was achieved. After steady state operation was achieved the oxygen balance calculated on the basis of the cell current and the measured inlet and outlet partial pressures of oxygen in seawater, as shown in Figure 5.1, was within experimental error.

5.3 Conclusions

This experiment indicates that the gill and fuel cell systems can be successfully integrated without unexpected results. Further development on both systems can, therefore, continue before they are integrated and characterized together without fear that such development will be undone by the integration.

6.0 ALUPOWER-ALWATT HYDROGEN GENERATOR

6.1 Purpose

This experiment was to check the power output and hydrogen output of the Alwatt Aluminum-Seawater Battery at the operating temperature of zero degrees Celsius.

6.2 Experimental Setup

The Alwatt battery was suspended in thirty gallons of Instant Ocean mixed to a refractive index corresponding to 33 PPT. The seawater tank was a fifty gallon trash can with a glass wool insulating blanket on the outside. The hydrogen exit of the battery runs to a Hoechst Celanese 20201040 polypropylene membrane cartridge containing three square meters of surface area with 40 percent porosity. The membrane module allows the hydrogen gas to flow through the membrane while leaving behind the foam created by the battery. A return form drain tube is used so the foam can return to the seawater battery. A Serria Allborg mass flow meter with a 0-200 ml/min range was used to measure the flow rate. The flow meter was calibrated with oxygen gas and corrected for hydrogen gas. It should be noted that the hydrogen was being produced at the temperature of the seawater tank and it was being measured at room temperature.

A Hewlett Packard 6825A power supply was used as the power sink for the battery output. Voltage was read from the voltage drop across the power sink and current was recorded from a shunt resistor (50 mV equals 5 amps). Data for the gas output, cell voltage and cell current was collected using the Aquanautics Ducksoup data collection system.

For future battery use it should be noted that the output leads to the battery are incorrectly colored so that black is positive and red is negative.

6.3 Procedure

Four sets of data were taken during this experiment:

- The battery was run initially in a short circuit configuration to evaluate the start-up profile and to see how much power could be extracted from the system. The time of this experiment was about three hours.
- The second set of experiments was a current vs. voltage profile run at 4.4 degrees Celsius.
- Next the cell was run at a constant current based upon the hydrogen generation output of the battery. This was to see how the system ran at the desired design point based on hydrogen output. Here the voltage profile as well as the hydrogen output was measured over time. This experiment was run for 19 hours. The temperature rose 6.2 degrees Celsius over the course of the data collection.
- The last set-up change was a repeat of the second experiment where the voltage current profile is examined. For the second current voltage profile the seawater temperature had risen to 10.6 degrees Celsius.

6.4 Results

The seawater battery was first run in a short circuit configuration with no voltage and maximum current. This phenomenon is shown in Figure 6.1.

Temperature seems to have the largest effect on the hydrogen output and current density of the cell. Figure 6.2 shows the results of the second and forth experiments. In Figure 2, the current-voltage profile is shown for two different temperatures. Here the cell voltage for zero current is the same. However, as the cell approaches a short circuit, the current output from the battery is more than twenty-five percent higher.

In the third set of data, the voltage is recorded at a constant current for nineteen hours. During this time the current is fixed at 0.23 amps. The cell voltage starts at 1.58 volts and rises to 1.66 volts. The corresponding temperature change for the same period is 4.4 degrees Celsius to 10.6 degrees Celsius. The hydrogen output corresponds to the current and does not seem to be temperature related, except that temperature does affect the current voltage profile.

An example of this is depicted in Figure 6.3. This is the hydrogen vs. current profile for the two different temperatures. It should be noted that the time period of data collection is different for the two experiments. This is represented in the data scatter of the lower temperature experiment in Figure 6.3. Here the data for the first experiment, at the lower temperature, was averaged over a shorter time period than the last set of data.

6.4 Conclusions

Once the cell has reached its initial peek operating performance for a given temperature, the temperature of the seawater seems to be the biggest variable in the battery performance. The initial start up of time of the cell seems to slow, about three hours. The temperature change of the seawater during the start-up period, does not account for much of the rise in the current during the start-up period.

Figure 6.1

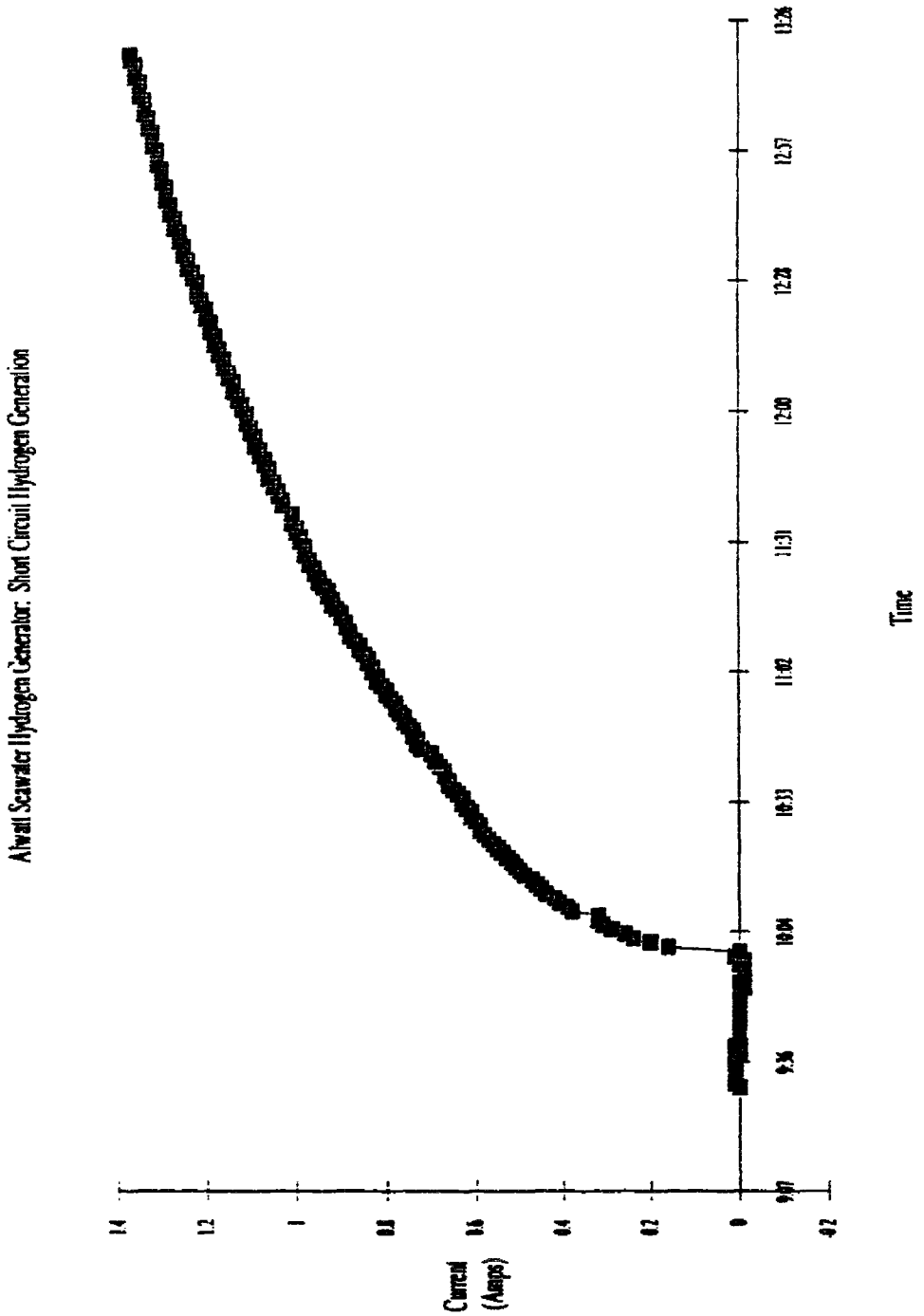
Alwall Seawater Hydrogen Generator. Short Circuit Hydrogen Generation
Current (Amps)
1.4
1.2
1
0.8
0.6
0.4
0.2
0
-0.2
Time
12:26
12:57
12:28
12:00
11:31
11:02
10:33
10:04
9:36
9:07

Figure 6.2

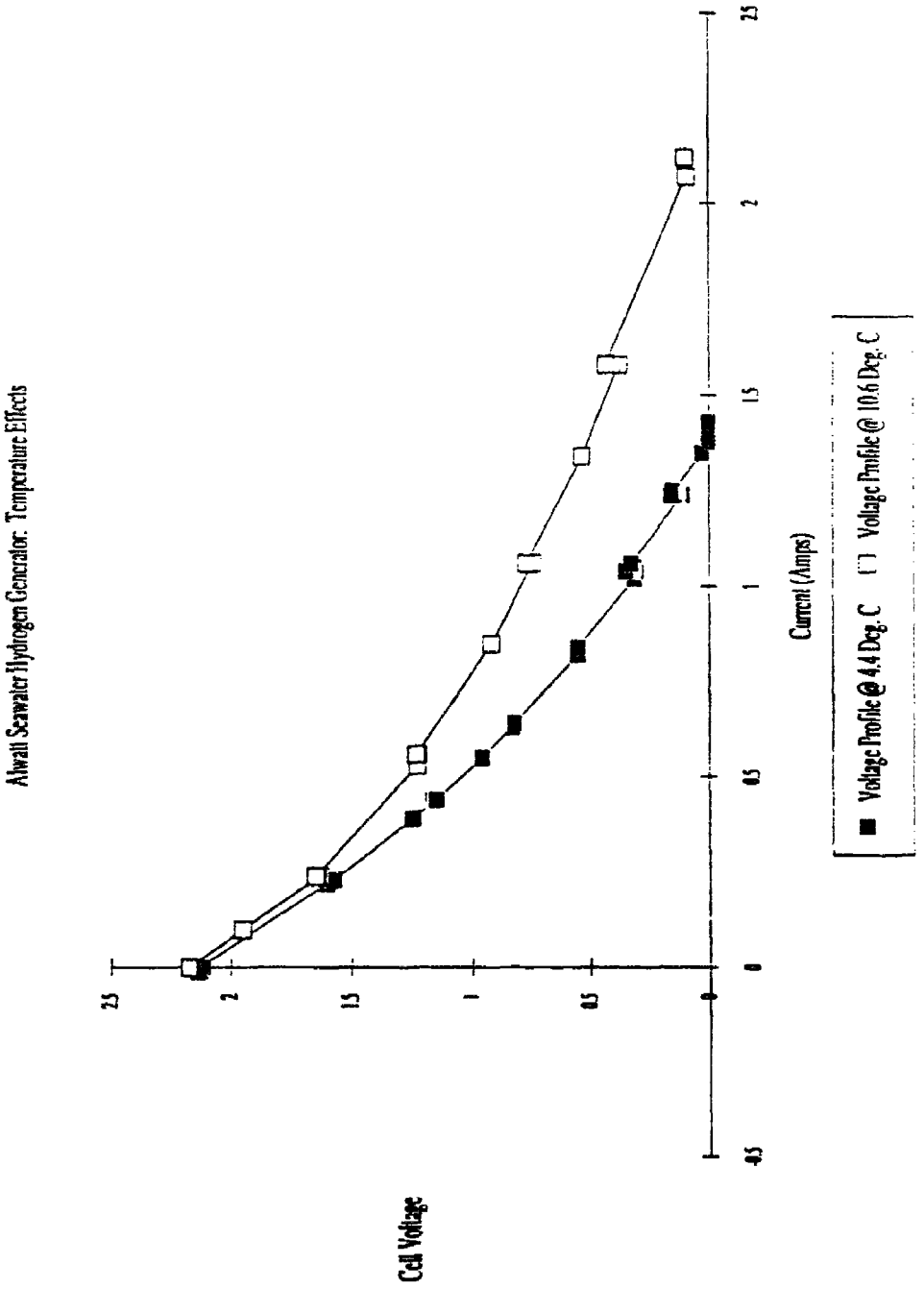
Alwali Seawater Hydrogen Generator: Temperature Effects
Cell Voltage
Current (Amps)
2.5
2
1.5
1
0.5
0
-0.5
Voltage Profile @ 4.4 Deg. C
Voltage Profile @ 10.6 Deg. C

Figure 6.3

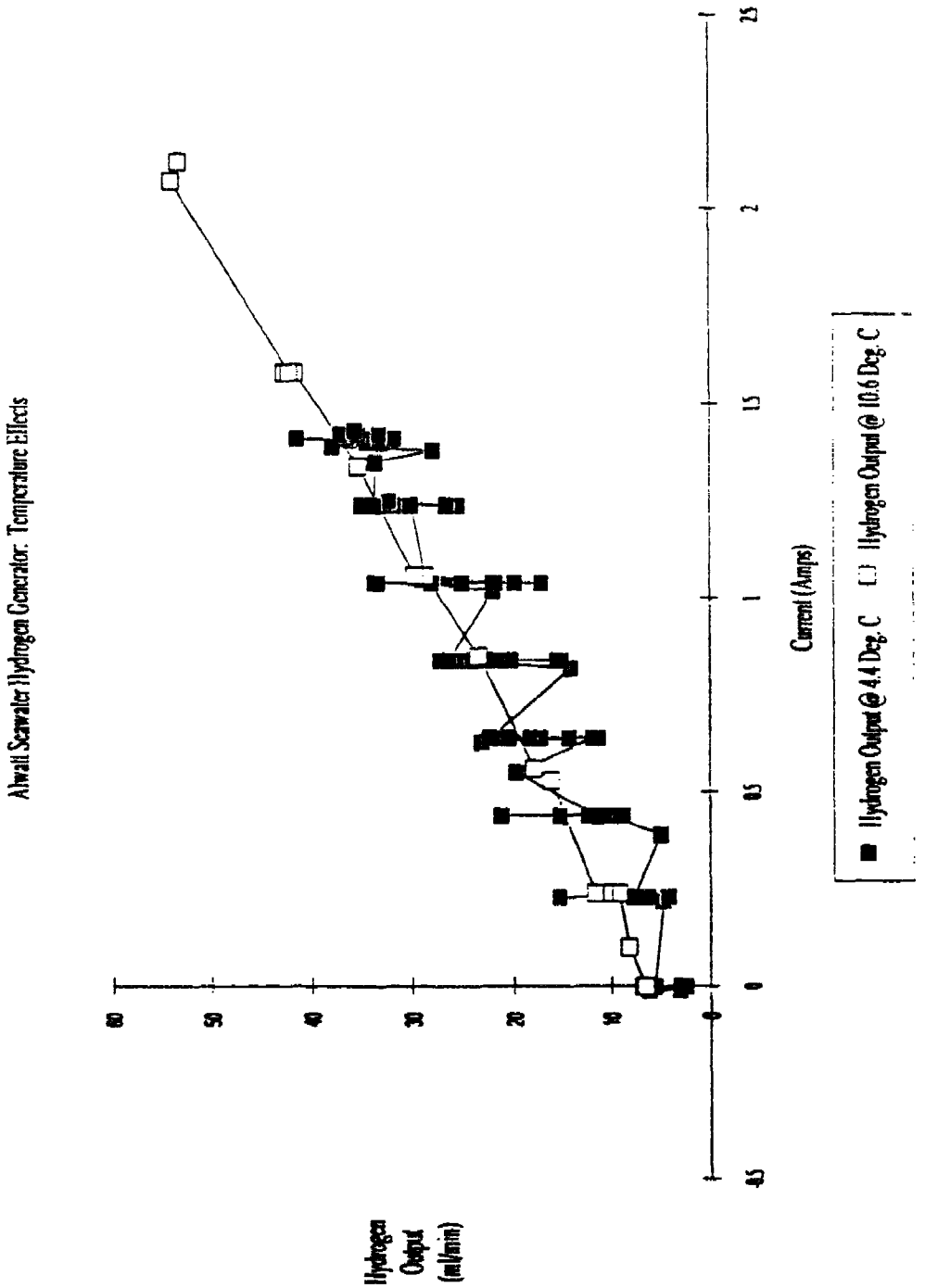
Alwall Seawater Hydrogen Generator: Temperature Effects
Hydrogen Output (ml/min)
60
50
40
30
20
10
0
Current (Amps)
0
0.5
1
1.5
2
2.5
4.5
Hydrogen Output @ 4.4 Deg. C
Hydrogen Output @ 10.6 Deg. C

7.0 CARRIER

7.1 Summary

6 EOCs were operational, 3 with pure O_2 output. The best lifetime is 6 weeks.

7.2 Objectives

1. Install one more MP cell-sized EOC and complete installation of "kinetics EOC". Operate at least 3 MP cell systems in the pure O_2 unload mode and modify unloaders to optimize for this output mode.
   Status: completed except for kinetics rig for which there has been no demand.

2. Repeat pure O_2 lifetime study on 23SP. Compare with an air unload control.
   Status: experiments nearing completion.

3. Continue to screen at least one new carrier per month.
   Status: completed. Five new compounds screened in EOC this quarter.

4. Purify carriers for current efficiency comparison purposes.

5. Design and build in conjunction with L'Air Liquide long-term EOCs.
   Status: on hold.

6. Test new GDE cell system.
   Status: on hold.

7.3 Other Achievements

Preparation of a new mediator has been accomplished and the compound functions well. It has shown good capability for catalysis with 23SP and has enabled the power requirement to be reduced to less than 150 $WminL^{-1}$.

1. We now have six operating EOCs, two of which have 25 cm^2 cells and four have 100 cm^2 MP cells. Of the four larger size systems, three are capable of continuous operation in the pure O_2 unload mode with reasonable accuracy. We have two 10 ml/min and one 20 ml/min flowmeters and two further 50 ml/min flowmeters. Since the accuracy is not good below 10% full scale, our lower limit for output is thus 1 ml/min. The present unloaders appear to operate satisfactorily at the current oxygen outputs. Further design changes will be implanted.

2. One experiment has been completed using 23SP plus mediator in an EOC in the air unload mode. The carrier lasted for six weeks before failing. Another experiment has been underway for four weeks using similar carrier conditions but with a pure O_2 unloading mode. The experiment is not yet complete.

3. During the period, 3 new compounds have been screened, 2SP, 3SP and 232NP.

4. Experiments with 23SP have been performed where the HCl salt was recrystallized four times and carefully dried. This material gave continuous performance with an electron count of less than 3. Another experiment using free base 23SP gave an electron count of closer to 4. This results in poorer power requirements and poorer

purity when the EOC is run in the pure O_2 unload mode. The steady-state electron count lifetime does not appear to be affected, however.

A new mediator has been screened. It performs as expected with 33SP giving the same performance as earlier mediators. When used with 23SP the power requirements dropped to less than 150 watt.min/L for almost four weeks and the useful lifetime of 23SP was extended to 6 weeks from 4 weeks.

During the course of support work for fuel cell experiments, some experiments with anions other than chloride were tried. The use of fluoride seemed to be acceptable, although the conductivity was lower. The use of perchlorate was disastrous, the solution rapidly polymerizing to give insoluble material. Both carbonate and acetate were tried. The latter functioned in the fuel cell but in the EOC a voltage of 1.2 volts was required to obtain oxygen from 23SP as opposed to 0.8 - 0.9 V with chloride. This indicates binding by acetate to the cobalt (III) form. Such observations are in line with our previous observations with ferrocene carboxylic acids and phosphate.

7.4 Objectives and Workplan for Next Quarter

1. Design, build and operate a small volume EOC requiring less than 50 ml. of solution. Design and build new loaders and unloaders to reduce present volumes by 50%.

2. Design, build and operate a battery of fuel cell test apparati to evaluate carriers for fuel cell operation.

3. Screen at least one new compound per month in the EOC and one per month in fuel cells. Operate at least three in the pure O_2 unload mode and achieve the longevity goal of 6 weeks operation at >90% oxygen purity at less than 200 watts per minute per liter.

4. Evaluate different electrode treatment procedures with respect to electrochemical kinetics. Prepare electrodes modified with catalysts and test. Initiate kinetics program with C. Amatore, obtain and operate basic simulation software.

5. Continue evaluation of carriers by cyclic voltammetry for stability and fuel cell function.

6. Revamp reporting procedures for EOC operations and carrier evaluations. Ensure that all EOC databases are up to date and complete.